

# AMERICAN MUSEUM *Novitates*

PUBLISHED BY THE AMERICAN MUSEUM OF NATURAL HISTORY  
CENTRAL PARK WEST AT 79TH STREET, NEW YORK, NY 10024  
Number 3525, 36 pp., 24 figures  
July 31, 2006

## Redescription and Phylogenetic Position of the Early Miocene Penguin *Paraptenodytes antarcticus* from Patagonia

SARA BERTELLI,<sup>1</sup> NORBERTO P. GIANNINI,<sup>2</sup> AND DANIEL T. KSEPKA<sup>3</sup>

### ABSTRACT

*Paraptenodytes antarcticus* is one of the best-known and most complete fossil penguins. This taxon is so distinctive that it has traditionally been classified in its own subfamily (Sphenisciformes: Paraptenodytinae) separate from all living penguins (Spheniscinae). The well-preserved partial skull of *P. antarcticus* is one of our richest sources of data on early penguin cranial morphology. We provide an updated description of the skull of *P. antarcticus* in a comparative context and use this information to explore the phylogenetic relationships of this taxon. Three cladistic analyses using an osteology dataset, a larger morphological dataset (including osteological, soft tissue, behavior, and oological characters) and a combined (morphological + molecular) dataset all recover *Paraptenodytes* as the sister taxon to a clade including all extant penguins. The placement of *Paraptenodytes* outside the crown clade of extant penguins reveals the order in which many spheniscid synapomorphies were acquired and lends support to the hypothesis that modern penguins had Subantarctic ancestors.

### INTRODUCTION

*Paraptenodytes antarcticus* (Moreno and Mercerat, 1891) is a fossil penguin from the Early Miocene of Patagonia. The most complete specimen of this taxon, AMNH 3338, comprises the cranium, mandible, and much

of the postcranial skeleton. Such preservation is highly unusual among fossil penguins, the majority of which are known only from a few isolated postcranial elements. At the time of its discovery, AMNH 3338 was the most well-known fossil penguin and the only specimen with a reasonably complete skull. In the

<sup>1</sup> Division of Invertebrate Zoology (Ornithology), American Museum of Natural History; Department of Vertebrate Paleontology, Natural History Museum of Los Angeles County (sbertelli@amnh.org).

<sup>2</sup> Division of Invertebrate Zoology (Mammalogy), American Museum of Natural History (norberto@amnh.org).

<sup>3</sup> Division of Paleontology, American Museum of Natural History (dksepka@amnh.org).

decades since Simpson (1946) described the specimen, several new sphenisciform skulls have been unearthed (Marples, 1960; Stucchi, 2002; Stucchi, 2003; Acosta Hospitaleche and Canto, 2005; Slack et al., 2006), but that of AMNH 3338 remains one of the most important, particularly given its unique morphology. The skull preserves a mixture of putatively primitive characters, synapomorphies shared with extant penguins, and features unique to *Paraptenodytes*.

Simpson (1946) described the most important features of the cranium of AMNH 3338 and compared the postcranial elements to those of other fossil and living penguins. He considered *Paraptenodytes* so different from other penguins that he erected a new subfamily (Paraptenodytinae) to accommodate it. This subfamily was accepted by subsequent workers including Marples (1962) and Brodkorb (1963), but Simpson (1976) later considered formal division of penguins into subfamilies unfeasible given available information. Regardless, these classifications were all precladistic, and the relationships of *Paraptenodytes* have never been investigated in a phylogenetic context.

Simpson (1946) described AMNH 3888 in a landmark contribution to the study of fossil penguins. Though Simpson's comparison of the postcranium with other fossil and living penguins was thorough, his description of the skull was quiet brief and neglected many key features. In light of the recent resurgence of interest in penguin relationships (e.g., Giannini and Bertelli, 2004; Bertelli and Giannini, 2005; Baker et al. 2006) and multiple new fossil discoveries from South America (e.g., Stucchi, 2002; Clarke et al., 2003; Acosta Hospitalache and Canto, 2005), a revised treatment of *Paraptenodytes* is in order. In this contribution, we provide a thorough redescription of the cranium and mandible of AMNH 3338 in a comparative context. We scored AMNH 3338 using the dataset of Bertelli and Giannini (2005), which included a dense outgroup and all living penguin species. On the basis of a cladistic analysis of the modified character set consisting of 159 morphological and behavioral characters and sequence fragments from two mitochondrial genes (12S and cytochrome *b*),

we propose a phylogenetic placement for *Paraptenodytes* and examine the implications of this fossil in the biogeographic history of the penguin clade.

## METHODS

**OSTEOLOGICAL DESCRIPTION:** We provide here a complete redescription of the skull of *Paraptenodytes antarcticus* AMNH 3338. Anatomical nomenclature follows Baumel et al. (1993) except when noted. The Latin terminology used by Baumel et al. (1993) is retained for muscles and ligaments, and osteological structures are described with English equivalents of the Latin terms (although the Latin equivalent is also given).

**TAXA:** The most complete specimen of *Paraptenodytes antarcticus* (AMNH 3338: Figures 1–21), includes an incomplete skull (see below), nine vertebrae (atlas, axis, presumed 6th, 8th, 11th, and 13th cervicals, and first three dorsals), the right anterolateral margin of the sternum, the cranial ends of the both scapulae, both coracoids, both humeri, the proximal end of the right and distal end of the left femur, the proximal end of the right and distal end of the left tibiotarsus, and the near complete left and partial right tarsometatarsi. Other referred specimens assigned to *P. antarcticus* do not contribute additional elements with certainty (Simpson, 1946). We included AMNH 3338 in a cladistic analysis with the same taxonomic representation as Bertelli and Giannini (2005), which included 11 outgroup taxa from representative Gaviiformes (*Gavia stellata*) and Procellariiformes (*Dioemedea melanophrys*, *Phoebetria palpebrata*, *Macronectes giganteus*, *Daption capense*, *Pterodroma incerta*, *Puffinus gravis*, *Procellaria aequinoctialis*, *Pachyptila desolata*, *Oceanites oceanicus*, *Oceanodroma leucorhoa*, and *Pelecanoides urinatrix*), as well all 17 currently recognized extant penguin species and one distinct subspecies (*Aptenodytes forseri*, *A. patagonicus*, *Eudyptes chrysocome chrysocome*, *E. chrysocome moseleyi*, *E. chrysolophus*, *E. pachyrrhynchus*, *E. schlegeli*, *E. sclateri*, *E. robustus*, *Eudyptula minor*, *Megadyptes antipodes*, *Pygoscelis adeliae*, *P. antarctica*, *P. papua*, *Spheniscus demersus*, *S. humboldti*, *S. magellanicus*, and *S. mendiculus*).

**CHARACTERS:** Bertelli and Giannini (2005) generated a matrix of 159 characters from the osteology (70 characters), myology (15), digestive tract (1), integument (66), and breeding traits including behavior and oology (7 characters) of extant penguins. They also compiled published sequences from the 12S rDNA and cytochrome *b* (see GenBank Accession numbers and sequence representation in Bertelli and Giannini, 2005). To that dataset (with the addition of one osteological character modified from Mayr, 2005), we incorporated the applicable scorings obtained from *Paraptenodytes antarcticus* AMNH 3338 (see Results and Discussion below). The modified character list is given in Appendix 2.

**CLADISTIC ANALYSES:** We conducted three separate analyses. First, we ran a parsimony analysis using only the osteological characters from the morphological dataset. We ran 200 replications (saving up to 10 trees per replication) followed by TBR branch swapping and an extra TBR round on each of the optimal trees. We then ran a second analysis using the same search strategies but incorporating the entire morphological dataset (including soft tissue and breeding characters). For both morphological analyses we used the program TNT (Goloboff et al., 2004). Third, we conducted a combined analysis of molecular + nonmolecular data using the method of Direct Optimization (DO; Wheeler, 1996). In this approach, the transformation cost of unaligned sequences on a topology is calculated by way of optimization. At any given internal node of a candidate tree, a hypothetical ancestral sequence is created on the basis of the sequence of the two descendants, optimally inserting gaps whenever descendants differ in sequence length, and simultaneously accounting for substitutions. Costs of each transformation type (indel or substitution) are established a priori. According to these costs, the length of the tree is calculated as the sum of transformations on each internal node implied in the downpass optimization of the tree. The tree or trees that minimize this total cost are chosen. In practice, this is done by way of tree building and branch swapping; that is, examining a large number of candidate trees from many different starting points—just as in conventional parsimony analysis. Such

searches were run in the program POY 3.0.11 (Wheeler et al., 2003). We followed the search strategy of Giannini and Simmons (2003), also used in the combined analysis of penguins on which the present dataset is based (Bertelli and Giannini, 2005). Briefly, the molecular morphological data were optimized together in each candidate tree generated from 200 independent builds using random addition sequence of taxa (RAS). The optimal trees from each such replication were submitted to tree fusing (Goloboff, 1999). The parsimony ratchet (Nixon, 1999) was also employed, starting from topologies yielded from the previous stages (see details in Giannini and Simmons, 2003). Iterative pass optimization (IPO; Wheeler, 2003) was applied in all search stages. Bremer support values were calculated as implemented in POY (Wheeler et al., 2003).

## DESCRIPTION

### THE SKULL OF *PARAPTENODYTES ANTARTICUS*

The preserved portions of the skull of *Paraptenodytes antarcticus* AMNH 3338 include the braincase, caudal and dorsal parts of orbit, occiput, left and right otic regions, basicranium, right quadrate, articular end of the right mandible, and a fragment of the left mandibular ramus. The exact size of the skull is uncertain because of incompleteness. The cranium is 80 mm in length as measured between the *prominentia cerebellaris* and the rostral preserved portion of the frontal. The distance between external borders of the *fossae g. nasalis* (interorbital area) is 16 mm. The width at the zygomatic processes is 62 mm.

**FRONTAL REGION, ORBIT, AND TEMPORAL REGION:** AMNH 3338 retains most of the interorbital region and frontals (fig. 1). In the caudal part of the frontal region, a shallow depression (*depressio frontalis*) separates the two slight prominences. In extant penguins, this depression is part of a continuous and shallow longitudinal concavity, whereas in *Paraptenodytes*, the caudal depression is clearly separated from the slightly depressed interorbital area. The supraorbital margins of the frontals preserve the salt-gland fossa (*fossa glandulae nassalis*), but as Simpson (1946) noted, they lack the supraorbital shelf of the frontal (supraorbital ridge of Pycraft, 1898)

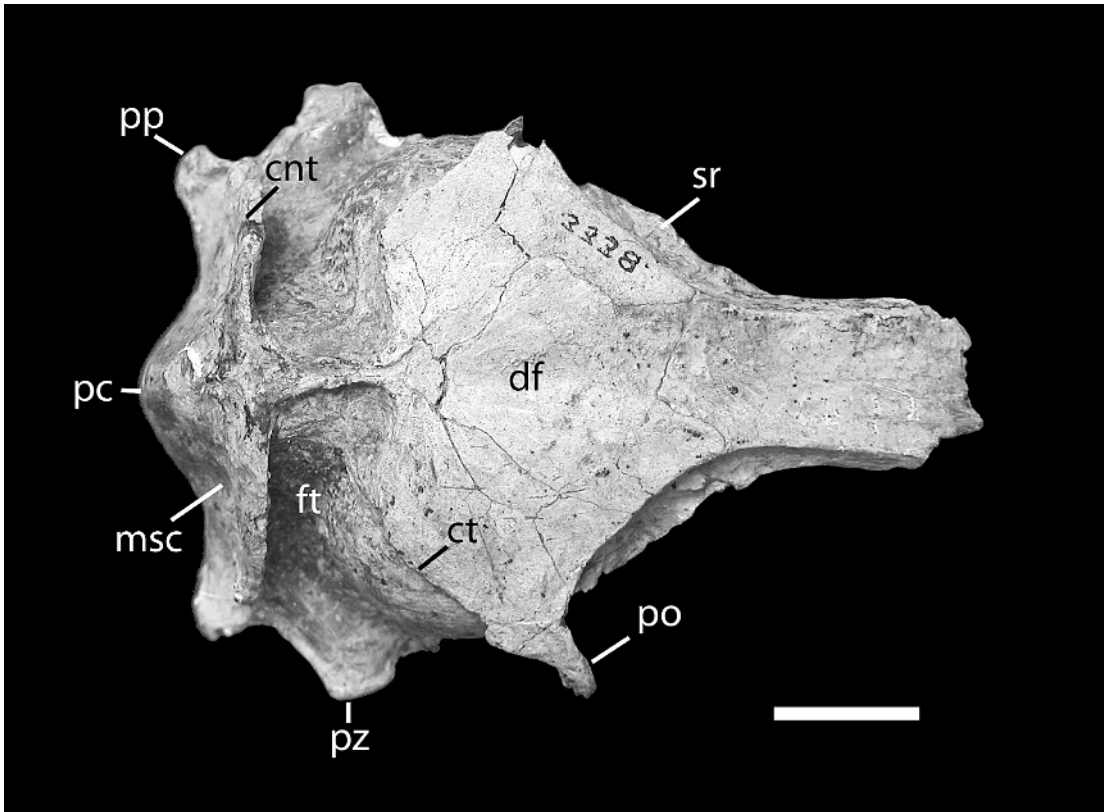


Fig. 1. Skull of *Paraptenodytes antarcticus* (AMNH 3338) in dorsal view. Abbreviations: cnt, crista nuchalis transversa; ct, crista temporalis; df, depressio frontalis; ft, fossa temporalis; msc, attachment area for the *m. splenius capitis*; pc, prominentia cerebellaris; po, processus postorbitalis; pp, processus paroccipitalis; pz, processus zygomaticus; sr, supraorbital ridge. Scale bar = 1 cm.

that bounds the salt gland laterally in some penguins. Ventrally, a small portion of the mesethmoid remains attached to the frontals (fig. 2). The *foramina n. olfactorii* open into grooves along the ventral surfaces of the frontals on either side of the mesethmoid (fig. 3). The caudal wall of the orbit is not perforated by *fonticuli orbitocraniales*. One of the most notable differences with respect to living penguins in this region of the skull is the configuration of the origin of the *m. pseudo-temporalis superficialis* on the *area muscularis aspera* (orbital surface of the laterosphenoid; fig. 4). The origin in *Paraptenodytes* is clearly divided into two separate surfaces by a longitudinal crest, creating a ventral surface situated on the caudal wall of the orbital cavity and a dorsal surface bounded by the *processus postorbitalis* and the caudal margin of the salt-

gland fossa. In contrast, a single attachment surface occupies this entire region in extant taxa. The ventral portion of the attachment site is much deeper in the fossil than any living form. At the base of the caudal wall of the orbit, the borders of the *foramen opticum* are irregular in outline, and the *foramina ethmoidale* are intact.

Simpson (1946) observed that the temporal fossae (*fossae temporales*) were strongly developed, extending dorsally almost to the sagittal plane and squarely abutting a longitudinal crest (fig. 1). Strong development of the temporal fossa is seen in all known fossil penguin skulls (e.g., *Marplesornis novaezealandiae* [Marples, 1960], *Waimanu tuatahi* [Slack et al. 2006], fossils assigned to the genus *Palaeospheniscus* [Acosta Hospitaleche and Canto, 2005], an unnamed Eocene fossil

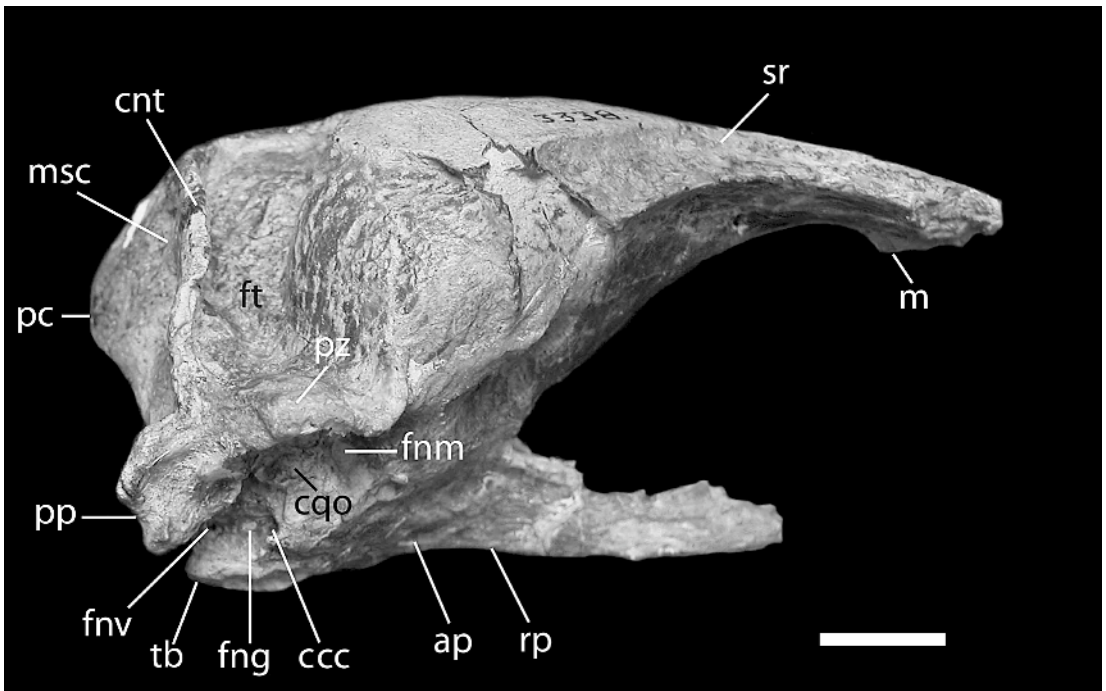


Fig. 2. Skull of *Paraptenodytes antarcticus* (AMNH 3338) in lateral view. Abbreviations: ap, foramen for the arteria palatina; ccc, canalis caroticus cranialis; cnt, crista nuchalis transversa; cqo, cotyla quadratica squamosi; fng, foramen n. glossopharyngealis; fmv, foramen nervi maxillomandibularis; fmv, foramen nervi vagi; ft, fossa temporalis; m, os mesethmoidale; msc, attachment area for the medial part of *m. splenius capitis*; pc, prominentia cerebellaris; pp, processus paroccipitalis; pz, processus zygomaticus; rp, rostrum parasphenoidale; sr, supraorbital ridge; tb, tuberculum basilare. Scale bar = 1 cm.

from Antarctica [Ksepka and Bertelli, in press], *Spheniscus urbanai* [Stucchi, 2002], and *S. megarhamphos* [Stucchi et al., 2003]. However, among living taxa, only *Spheniscus* approaches this degree of development. The left and right temporal crests (*cristae temporales*) closely approach one another between the temporal fossae, forming an extended sagittal crest (*crista nuchalis sagitalis*). The temporal crest reaches rostrally onto the base of the postorbital process (*processus postorbitalis*), preserved on the right side. This crest contacts the transverse nuchal crest (*crista nuchalis transversa*) at a nearly right angle. The transverse nuchal crest is nearly perfectly aligned to the coronal plane in *Paraptenodytes*, whereas in other living and fossil penguins this crest curves posterolaterally. Ventrally, the transverse nuchal crest divides in two segments; the rostral segment extends to the zygomatic process (*processus*

*zygomaticus*) and the caudal segment extends to the paroccipital process (*processus paroccipitalis*) (fig. 2). The subtemporal fossa (*fossa subtemporalis*, origin of *m. depressor mandibulae*) is located ventrally between the rostral and caudal divisions of the transverse nuchal crest (fig. 5). This fossa is deeply excavated in *Paraptenodytes*, contrasting with the nearly flat surface seen in living penguins.

**OCCIPUT, CRANIAL BASE, AND MIDDLE EAR:** Simpson (1946) described the subcircular shape of the cranium in posterior view (fig. 5). This shape is caused primarily by the caudolateral arching of the dorsal and lateral borders of the transverse nuchal crest. The crest arches more sharply ventrally in living forms, giving the skull a more rhomboid outline. The paroccipital process is bifid, with a ventral and a dorsolateral projection. Simpson (1946) noted the uniqueness of this structure compared to the blunt, undivided

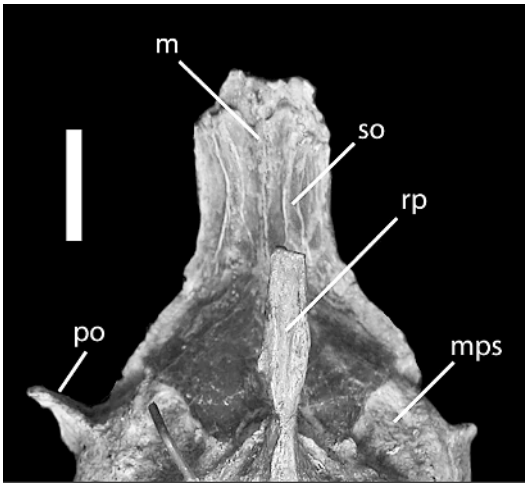


Fig. 3. Closeup of the rostral portion of the cranium of *Paraptenodytes antarcticus* (AMNH 3338). Abbreviations: m, os mesethmoidale; mps, attachment area for *m. pseudotemporalis superficialis*; po, processus postorbitalis; rp, rostrum parasphenoidale; so, sulcus for n. olfactori. Scale bar = 1 cm.

paroccipital process of other fossil and living penguins. The borders of the process are thicker in *Paraptenodytes* than in extant taxa. Dorsolateral to this structure, and adjacent to the transverse nuchal crest, there is a small fossa that corresponds to the location of the *foramen rami occipitalis arteriae ophthalmicae externae* (best observed on the left side). The cerebellar prominence (*prominentia cerebellaris*) is relatively smaller in *Paraptenodytes* than in any living form (Simpson, 1946). A slight median crest (*crista nuchalis sagittalis*) surmounts the dorsal surface of the cerebellar prominence, a feature also developed in extant *Spheniscus*. In *Paraptenodytes*, the *crista nuchalis sagittalis* is clearly confluent with the *crista nuchalis transversa*. On either side of the prominence and on the posterior surface of the paroccipital process, there are depressed circular areas that we interpret as the surfaces for the attachment of the *m. splenius capitis*. Both are deeper than in any recent form (especially the surface on the paroccipital

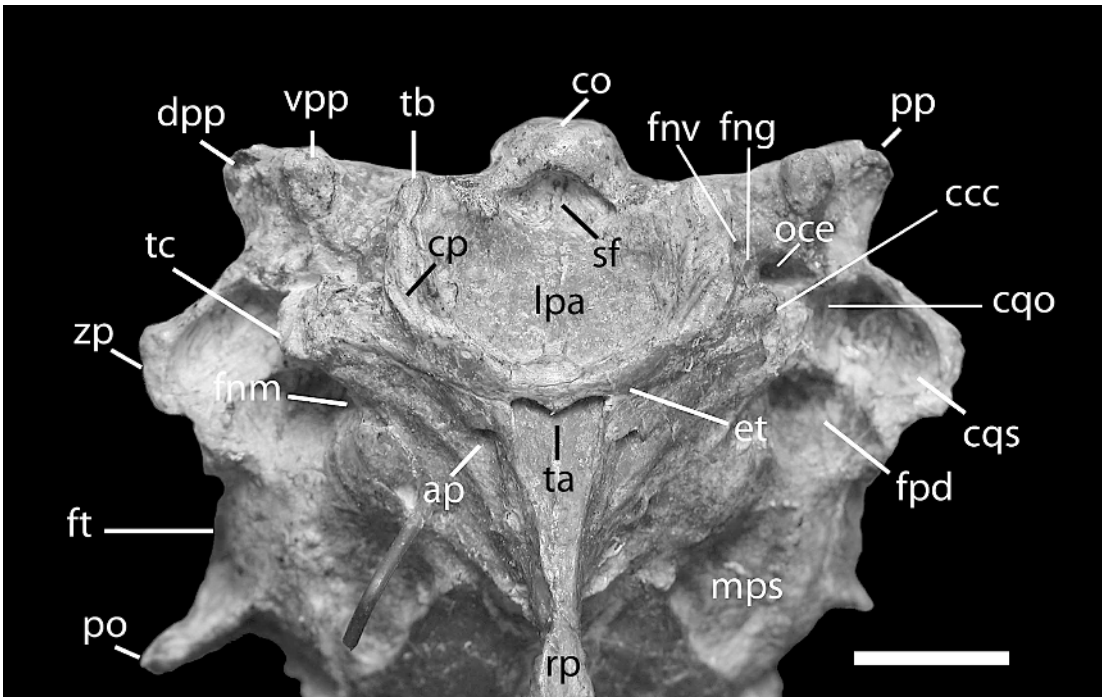


Fig. 4. Close-up of the basicranium of *Paraptenodytes antarcticus* (AMNH 3338). Abbreviations: ap, foramen for the arteria sphenoidale; ccc, ostium canalis carotici; co, condylus occipitalis; cp, capping pad on the lateral process of the basitemporal plate (basitemporal articulation of the mandible; Bock, 1960); cco,

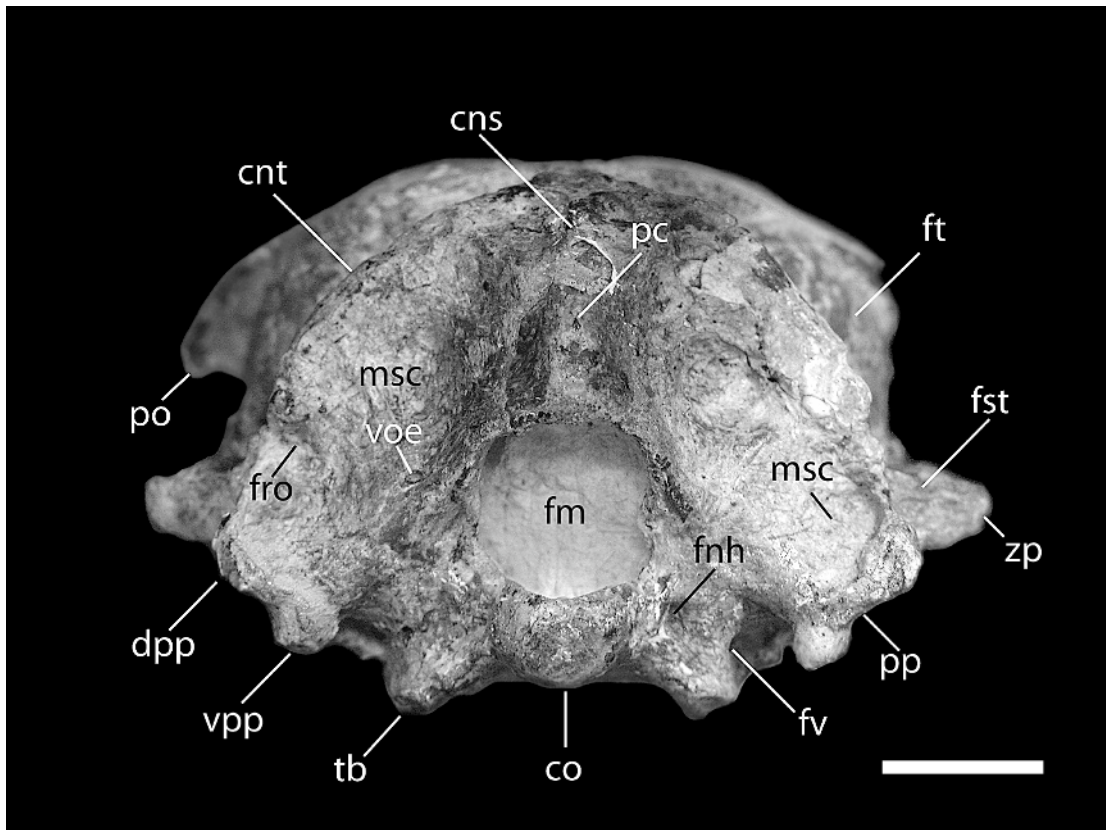


Fig. 5. Skull of *Paraptenodytes antarcticus* (AMNH 3338) in occipital view. Abbreviations: cns, crista nuchalis sagittalis; cnt, crista nuchalis transversa; co, condylus occipitalis; dpp, dorsolateral projection of the processus paroccipitalis; fnh, foramen nervi hypoglossi; fm, foramen magnum; fro, foramen rami occipitalis arteriae ophthalmicae externae; fst, fossa subtemporalis; ft, fossa temporalis; fv, foramen nervi vagi; msc, attachment area for the *m. splenius capitis*; pc, prominentia cerebellaris; po, processus postorbitalis; pp, processus paroccipitalis; tb, tuberculum basilare; voe, foramen venae occipitalis externae; vpp, ventral projection of the processus paroccipitalis; zp, processus zygomaticus. Scale bar = 1 cm.

process). The *venae occipitalis externae* exits through a small foramen on either side of the foramen magnum, lateral to the paroccipital process (preserved on the left side). This foramen is expanded into a sulcus in some extant penguins.

The occipital condyle (*condylus occipitalis*) is circular in shape. Anterior to the condyle is a deep, sharply defined subcondylar fossa (*fossa subcondylaris*) (Simpson, 1946). The opening for cranial nerve XII (*foramen nervi hypoglossi*) is preserved lateral to the condyle

←

cotyla quadratica otici; cqs, cotyla quadratica squamosi; dpp, dorsolateral projection of processus paroccipitalis; et, tuba auditiva; fng, foramen nervi glossopharyngealus; fnv, foramen nervi vagi; fnm, foramen nervi maxillomandibularis; fpd, foramen pneumaticum dorsale; ft, fossa temporalis; lpa, lamina parasphenoidalis; mps, attachment area for *m. pseudotemporalis superficialis*; oce, ostium canalis ophthalmici externi; po, processus postorbitalis; pp, processus paroccipitalis; rp, rostrum parasphenoidale; sf, fossa subcondylaris; ta, tuba auditiva communis; tb, tuberculum basilare; tc, tympanic cavity (Saiff, 1976); vpp, ventral projection of the processus paroccipitalis; zp, processus zygomaticus. Scale bar = 1 cm.

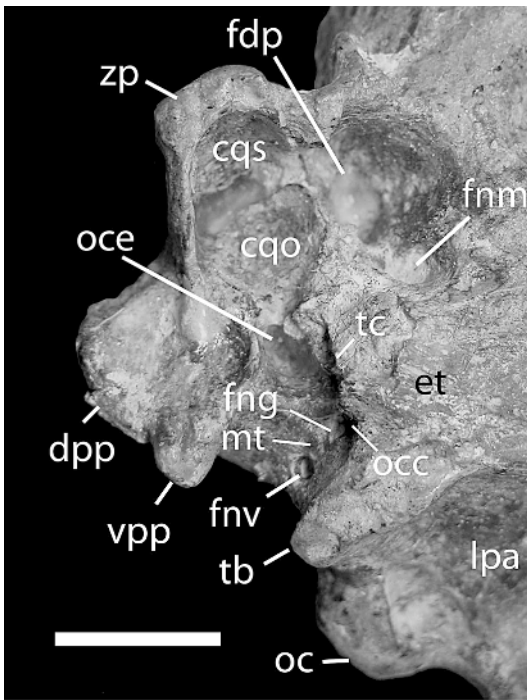


Fig. 6. Close-up of the right middle ear region of *Paraptenodytes antarcticus* (AMNH 3338). Abbreviations: cqs, cotyla quadratica otici; cqs, cotyla quadratica squamosi; dpp, dorsolateral projection of processus paroccipitalis; et, tuba auditiva; fng, foramen nervi glossopharyngeus; fmv, foramen nervi vagi; fnm, foramen nervi maxillomandibularis; fdp, foramen pneumaticum dorsale; lpa, lamina parasphenoidalis; mt, metotic process (Saiff, 1976); oc, condylus occipitalis; occ, ostium canalis carotici; oce, ostium canalis ophthalmici externi; tb, tuberculum basilare; tc, tympanic cavity (Saiff, 1976); vpp, ventral projection of the processus paraoccipitalis; zp, processus zygomaticus. Scale bar = 1 cm.

on both sides. The concave and rhombic parasphenoid plate (*lamina parasphenoidalis*) has a pair of blunt and weak basal tubercles (*tuberculum basilare*) at its caudal corners. Simpson (1946) described the tubercles as low, but both are incomplete, so their degree of development is uncertain. The medial process of the mandible articulates with a capping pad on the lateral process of the parasphenoid plate (basitemporal articulation of the mandible; Bock, 1960). The eustachian tubes (*tubae auditivae*) traverse the rostrolateral border of the parasphenoid plate enclosed in a bony

canal and open at the base of the *rostrum parasphenoidale*. The opening of the eustachian tubes in the otic cavity is not visible because the middle ear region is filled with sediment (fig. 6). The squamosal and otic cotylae (*cotylae quadratica squamosi et otici*) are clearly separated from the *foramen pneumaticum dorsale*. Medial to the otical cotyle, a large *foramen nervi mandibularis* is situated just anterior to the tympanic cavity. Pycraft (1898) and Saiff (1976) described the morphology of this region in living penguins. Posterior to the tympanic cavity, the openings for cranial nerves IX (*foramen nervi glossopharyngealis*) and X (*foramen nervi vagi*) are located in a poorly developed metotic process as described by Saiff (1976) in living penguins. The *foramen nervi vagi* is large and opens medial to the smaller *foramen nervi glossopharyngealis*. The *canalis caroticus cranialis* and *canalis ophthalmicus externus* are fully ossified, as in living penguins (Saiff, 1976).

**PTERYGOID:** The pterygoid of *Paraptenodytes* (fig. 7) is so different from that of living penguins that Simpson (1946:12) noted that, “[i]f the pterygoid ... had been found isolated it would never have been considered spheniscid but perhaps procellariiform” (cf. fig. 7 and fig. 7 in Bertelli and Giannini, 2005). The most obvious difference between *Paraptenodytes* and living penguins is the lack of expansion of the anterior portion of the pterygoid (*pes pterygoidei*) in the fossil. The *pes pterygoidei* is expanded laterally into a thin plate in all living penguins, giving the bone a subtriangular shape. *Marplesornis* also exhibits widened *pes pterygoidei* (Marples, 1960), but the degree of expansion is much less than that in extant penguins. In *Paraptenodytes*, a tablike process projects medially about one-third of the bone’s length from the anterior end. This feature is not seen in living penguins or *Marplesornis*. Simpson (1946) noted that the position of this process would suggest it was part of a basiptyergoid articulation, were it not for the absence of a corresponding articular surface on the parasphenoid rostrum. He speculated that this process possibly represented a nonosseous connection between the pterygoid and parasphenoid. A shallow, subcircular fossa is located at the posterior border of the base of the process. Two small articular



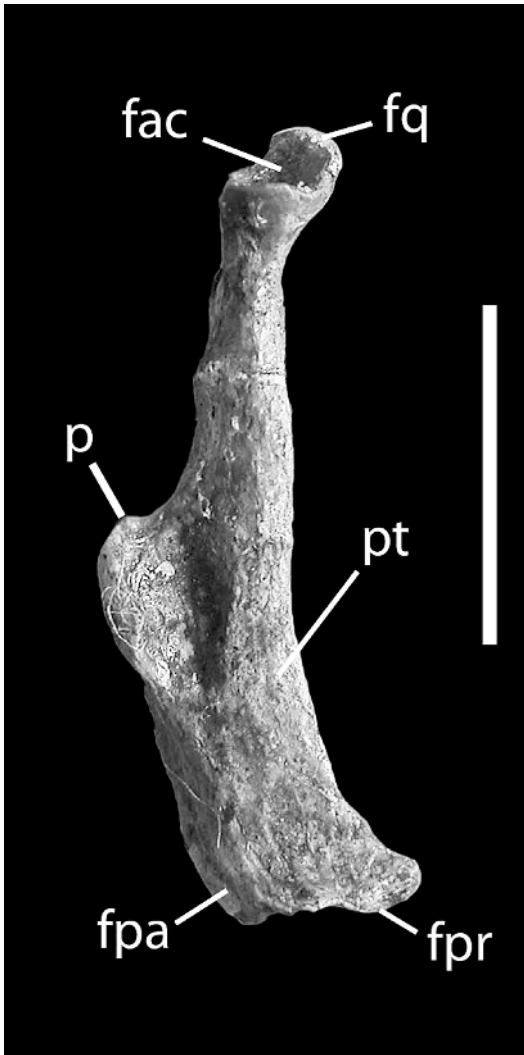


Fig. 7. Left pterygoid of *Paraptenodytes antarcticus* (AMNH 3338) in ventromedial view. Abbreviations: fac, facies articularis quadratica (for articulation with the condylus pterygoideus of the quadrate); fq, surface for articulation with the facies pterygoidea (Elzanowski et al., 2000) of the quadrate; fpa, facies articularis parasphenoidalis; fpr, facies articularis palatina; p, “tab-like medial process” of Simpson (1946); pt, pes pterygoidei. Scale bar = 1 cm.

surfaces, one for the parasphenoid rostrum (*facies articularis parasphenoidalis*) and one for the palatine (*facies articularis palatina*) are present at the anterior end of the *pes pterygoidei*. At the caudal end of the ptery-

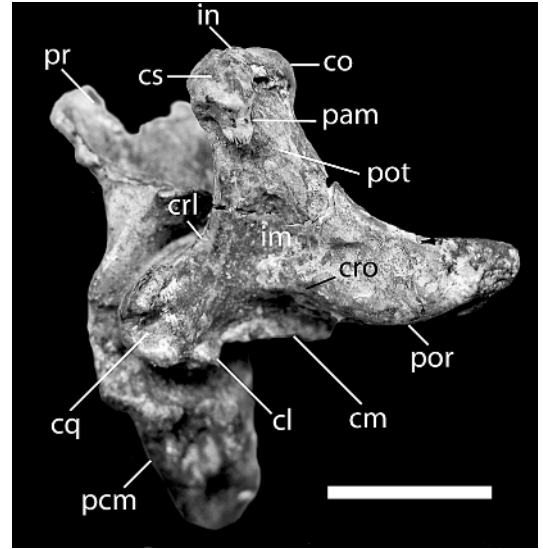


Fig. 8. Quadratum and articular area of the right mandible of *Paraptenodytes antarcticus* (AMNH 3338), in lateral view. Abbreviations: cl, condylus lateralis; cm, condylus medialis; co, capitulum oticum; cq, cotyla quadratojugalis; crl, crista lateralis (Elzanowski et al., 2000); cro, crista orbitocotylaris (Elzanowski et al., 2000); cs, capitulum squamosum; in, incisura intercapitularis; im, impressio for the insertion of the medial (deep) layers of the *m. protractor pterygoidei et quadrati* (Elzanowski et al., 2000); pam, processus for attachment of the *m. adductor mandibulae externus, pars profunda* (Hofer, 1950); pcm, ramus mandibulae, pars caudalis; por, processus orbitalis; pot, processus oticus; pr, processus retroarticularis. Scale bar = 1 cm.

goid, a rounded cotyla (*facies articularis quadratica*) serves as the articulation with the *condylus pterygoideus* of the quadrate. Dorsal to this cotyle, a facet forms a second articulation with the quadrate at the base of the orbital process.

**QUADRATE:** The right quadrate is complete (figs. 8 and 9). The quadrate was reattached to the mandible following Simpson's (1946) description, but most of the morphology remains observable. Simpson (1946: 12) provided only a few brief remarks on the general structure of the quadrate, noting it is “more stoutly constructed with a longer otic process than in any recent species.” On the articular surface of the otic process (*processus oticus*), a slightly larger squamosal capitulum (*capitulum squa-*

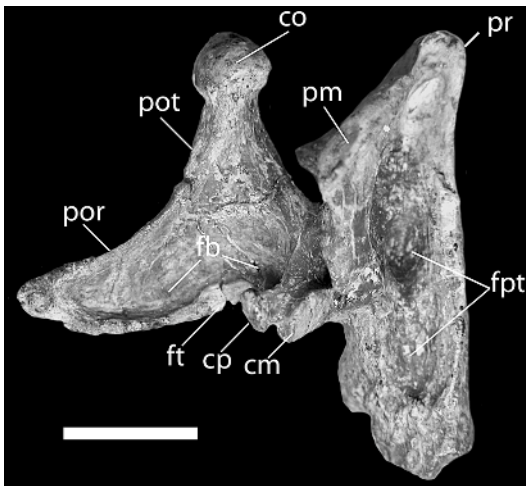


Fig. 9. Quadratum and articular area of the right mandible of *Paraptenodytes antarcticus* (AMNH 3338), in medial view. Abbreviations: cm, condylus medialis; co, capitulum oticum; cp, condylus pterygoideus; fb, fossa basiorbitalis (Elzanowski et al., 2000); fpt, fossa for insertion of *m. pterygoideus* (part O of Zusi, 1975); ft, facies pterygoidea (Elzanowski et al., 2000); pm, processus medialis mandibulae; por, processus orbitalis; pot, processus oticus; pr, processus retroarticularis. Scale bar = 1 cm.

*mosum*) projects farther dorsally than the otic capitulum (*capitulum oticum*). The intercapitular incisure (*incisura intercapitularis*) is shallow (fig. 8), whereas in the living penguins the capitula are separated by a deep incisure. In lateral view (fig. 9), the squamosal capitulum extends ventrally in a prominent hooklike tubercle for the attachment of the *pars profunda* of the *m. adductor mandibulae externus* (Hofer, 1950). In living penguins, this process is clearly separated from the squamosal capitulum. As noted by Simpson (1946), the orbital process (*processus orbitalis*) is longer than the otic process, the reverse of the condition found in living penguins. The lateral crest (*crista lateralis* of Elzanowski et al., 2000) for attachment of the tympanic membrane is sharp and extends from the lateral border of the squamosal capitulum to the quadratojugal cotyla (*cotyla quadratojugal*) (fig. 8). Adjacent to this crest, an impression located on the lateral side of the otic process near its transition to the body of the quadrate marks the probable attachment

of the medial (deep) layers of the *m. protractor pterygoidei et quadrati* (Elzanowski et al., 2000). There is no evidence of a medial crest (Fuchs, 1954; Elzanowski, 1987) or a tympanic crest on the medial or caudal surface of the otic process. The orbital process is concave medially and tapers toward its distal end. In medial aspect, the concavity deepens ventrally into the basiorbital fossa (Elzanowski et al., 2000), accommodating the insertion of the lateral (superficial) layers of the *m. protractor pterygoidei et quadrati* (Elzanowski et al., 2000) (fig. 9). In lateral view, the base of the process is ventrally connected to the quadratojugal articulation by a distinctive orbito-cotylar crest (Elzanowski et al., 2000) ending on the surface of the quadrate body just before the quadratojugal cotyla (fig. 8). The orbito-cotylar crest and the ventral margin of the orbital process enclose a deep groove. The pterygoid condyle (*condylus pterygoideus*) is a round, knoblike process with a constricted base; it projects more anteromedially than the medial condyle (*condylus medialis*) (fig. 9). A pterygoid facet is located medially at the base of the orbital process (fig. 9). The quadratojugal articulation is a deep, rounded socket (fig. 8). Its caudal margin projects laterally well past the other surface of the rim. There is no sign of pneumatic foramina on the quadrate. The medial and caudal mandibular condyles (*condylus medialis* and *condylus caudalis*) are obscured by the attached mandible.

**MANDIBLE:** Three portions of the mandible are preserved in AMNH 3338: the articular ends of the right and left mandible and a fragment of the left mandibular ramus (figs. 9, 10, and 11). Simpson (1946) commented on very few aspects of the mandibular morphology. He described the quadrate articulation, noting its resemblance to *Pygoscelis* among living penguins. Also, he described the morphology of the “postarticular” bone, in particular the medial and “posterior” processes, as the greatest distinction of the fossil mandible. Finally, he mentioned that because the mandibular ramus was so crushed, its anatomy and identification were uncertain. However, the incomplete mandible does provide significant information and further comment is warranted.

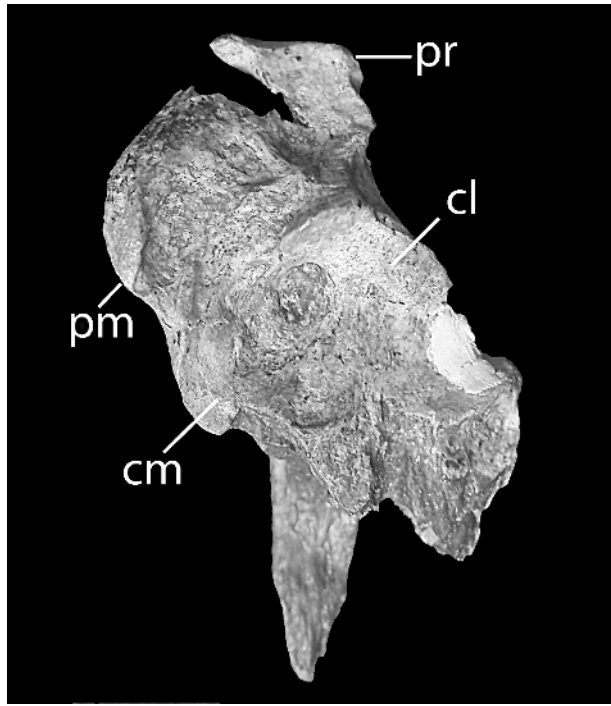


Fig. 10. Articular area of the left mandible of *Paraptenodytes antarcticus* (AMNH 3338) in dorsal view. Abbreviations: cl, cotyla lateralis; cm, cotyla medialis; pm, processus medialis mandibulae; pr, processus retroarticularis. Scale bar = 1 cm.

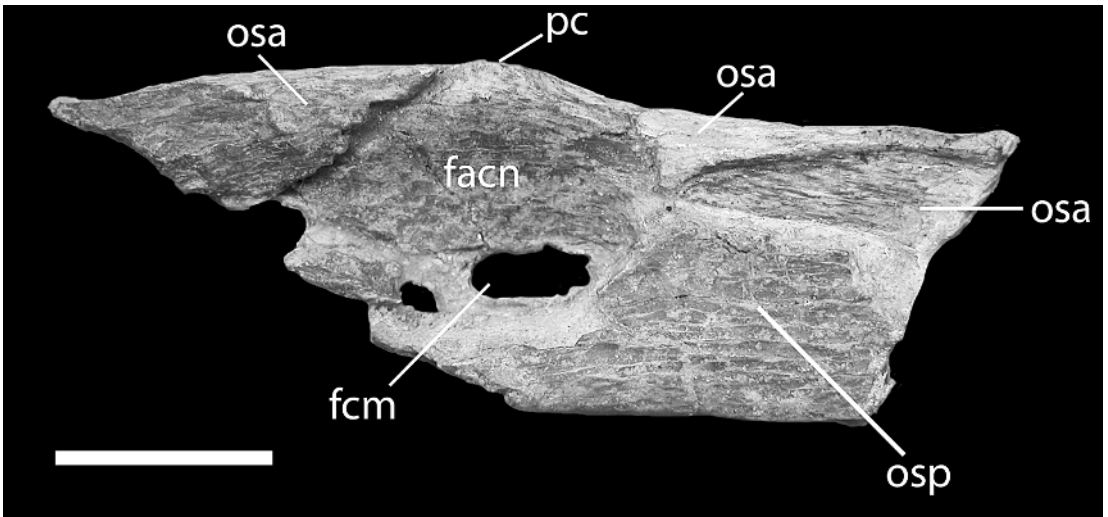


Fig. 11. Fragment of the left mandibular body of *Paraptenodytes antarcticus* (AMNH 3338) in medial view. Abbreviations: facn, fossa aditus canalis mandibulae; fcm, fenestra caudalis mandibulae; osa, os supra-angulare; osp, os prearticulare; pc, processus coronoideus. Scale bar = 1 cm.

The lateral and medial cotylae (*cotylae lateralis et medialis*) are well preserved on the articular area of the left mandible (fig. 10). The positions and shapes of the cotylae are in general similar in dorsal view to those in living penguins; we attribute apparent differences of the medial cotyla to breakage along the anteromedial margin. The most notable difference in *Paraptenodytes* is that the anterior and posterior margins of the lateral cotyla are more sharply projected. The fossa adjacent to the lateral cotyla is also deeper than in living penguins. As noted by Simpson (1946), there is no clear separation of the medial and retroarticular processes of the articular (*processus medialis mandibulae* and *processus retroarticularis*). The medial process is not projected and lacks the hooklike shape typical of all living penguins. The retroarticular process is wider and less projecting than in extant taxa, and the caudal fossa (*fossa caudalis*) is shallower. In living penguins, the medial and retroarticular processes are connected by a thin sheet of bone. The edge of this sheet of bone is a thin crest in living taxa, but is greatly thickened in *Paraptenodytes*. A wide groove separates the medial process from the medial cotyla. The depression for the insertion of the *m. pterygoideus* on the medial surface is extremely deep, much more so than in any living taxon. The features discussed above are also clear on the right mandible, except the cotylae are obscured by the articulated quadrate.

The lateral surface of the mandibular ramus is broken (fig. 11). In medial aspect, portions of the surangular (*os supra-angulare*), and prearticular (*os prearticulare*) are preserved. The caudal mandibular fossa (*fossa aditus canalis neurovascularis*) is large, as in other penguins. The caudal mandibular fenestra (*fenestra caudalis mandibulae*) is identifiable, but its borders are enlarged by breakage, so its true size is uncertain. The coronoid process (*processus coronoideus*) is weakly developed. The process must have been either posterior to or level with the caudal mandibular fenestra, though the exact position is uncertain. The prearticular lines the medial surface of the mandible, but the regions adjacent to the surangular and the caudal mandibular fossa are broken away. Dorsally the prearticular is

broken away, exposing the surangular in medial view.

#### SCORING OF *PARAPTENODYTES*

Thirty osteological characters from Bertelli and Giannini (2005) and one additional character from Mayr (2005) could be scored in *Paraptenodytes antarcticus* AMNH 3338. A discussion of this scoring follows.

**Character 73:** Basioccipital, subcondylar fossa (*os basioccipitale*, *fossa subcondylaris*): absent or shallow (0); deep (1). All extant penguins lack a distinct subcondylar fossa. The alternative condition—a deep fossa—is present in most outgroup taxa. *Paraptenodytes* exhibits a deep subcondylar fossa (fig. 4). Simpson (1946:11) noted this character state in AMNH 3338. This is one of the characters that contribute to place this form at the base of the penguin subtree (see below).

**Character 74:** Supraoccipital, paired grooves for the exit of the *v. occipitalis externa* (*os supraoccipitale*, *sulci venae occipitalis externae*): absent or poorly developed (0); deeply excavated (1). This structure is apparently not preserved in the right side of AMNH 3338. In the left side (fig. 5), the groove is inconspicuous (state 0), and the foramen for the *v. occipitalis externa* is placed lateral and adjacent to the foramen magnum.

**Character 75:** Frontal, salt-gland fossa (*os frontale*, *fossa glandulae nasalis*), lateral supraorbital shelf of bone: absent (0); present (1). *Paraptenodytes* lacks the lateral supraorbital shelf of the frontal (state 0; fig. 1) that bounds the salt gland laterally in some other penguins (state 1). The fossil AMNH 3338 allows for a positive scoring of this character, as the postorbital process on the left side appears complete and without the rostral extension that is associated with the shelf in the forms that possess it. Also, the salt-gland fossa (supraorbital groove of Simpson, 1946) is very narrow instead of expanded medially and laterally as when the shelf is present.

**Character 76:** Squamosal, temporal fossa (*os squamosum*, *fossa temporalis*), size: less extensive, both fossae separated by considerable cranial surface (at least the width of the cerebellar prominence) (0); more extensive, fossae meeting or nearly meeting at midline

of the skull (1). *Paraptenodytes* resembles *Spheniscus* in that the temporal fossa is deep and extends dorsally to midsagittal line (state 1; Simpson, 1946). The fossa is so excavated dorsally that a tall sagittal line is present (fig. 1).

**Character 77:** Squamosal, temporal fossa (*os squamosum*, *fossa temporalis*), depth of posterior region: flat (0); shallowly depressed (1); greatly deepened (2). *Paraptenodytes* shares a temporal fossa greatly deepened posteriorly (state 2; fig. 2) with several extant genera (except *Aptenodytes* and *Pygoscelis*; state 1).

**Character 79:** Orbit (*orbita*), *fonticuli orbitocraniales*: small or vestigial (0); broad and conspicuous (1). These openings in the caudal wall of the orbit communicate with the cranial cavity. They are invariably present and comparatively very large in *Aptenodytes* (state 1). In *Paraptenodytes*, the *fonticuli* are missing altogether, as in several old specimens of extant genera that possess small *fonticuli* (state 0).

**Character 86:** “Basitemporal plate” (*lamina parasphenoidalis*), dorsoventral position with respect to the occipital condyle: ventral to the level of the condyle (0); at the level of the condyle (1); dorsal to the level of the condyle, surface depressed (2). *Paraptenodytes*, as all extant penguins, exhibits a depressed *lamina parasphenoidalis* (state 2).

**Character 87:** Basipterygoid process: absent (0); vestigial or poorly developed (1); well developed (2). *Paraptenodytes*, as all penguins, lacks a basipterygoid process (state 0). Each side of the *rostrum parasphenoidale*, where the basipterygoid process would be located if present, is well preserved in AMNH 3338, so the absence of this process could be established positively (fig. 4). Simpson (1946) commented on the presence of an anterior medial facet (his pseudo-basipterygoid facet; see description above).

**Character 88:** Eustachian tubes (*tuba auditiva*): open or with very little bony covering near the medial end of the tube (0); mostly enclosed by bone (1). AMNH 3338 shows well-preserved left and right eustachian tubes (fig. 4). The tubes are long (state 1), reaching laterally to the otic cotylae (*cotylae quadratica otici*, the articulations for the otic capitulum of the left and right quadrate). The medial

openings of both tubes (on the ventral aspect of the base of the *rostrum parasphenoidale*) are also preserved in AMNH 3338. These openings are identical to the openings observed in extant penguins.

**Character 89:** Pterygoid (*os pterygoideum*), shape: elongated (0); broad, triangular-shaped (1). Unlike any other penguin for which the pterygoid is known, *Paraptenodytes* exhibits an elongated, approximately cylindrical pterygoid (state 0; fig. 7). Penguins in extant genera possess a pterygoid with a wide blade-like rostralateral flange (state 1). Simpson (1946) emphasized the distinctiveness of this bone in *Paraptenodytes*, much like the pterygoid of procellariiforms (most of our outgroup taxon set).

**Character 96:** Quadrate, otic process (*os quadratum*, *proc. oticus*), ventral border, process for attachment of the *m. adductor mandibulae externus, pars profunda* (Hofer, 1950): absent (0); present as a ridge (1); present as a tubercle or short process (2). The process is located on the rostralateral surface of the otic process of the quadrate, immediately ventral to the squamosal articulation (*capitulum squamosum*). The right quadrate of *Paraptenodytes* exhibits a prominent, hooklike process (state 2; fig. 8).

**Character 100:** Mandible, caudal fenestra (*mandibula, fenestra mandibulae caudalis*): open, can be seen through from the medial or lateral aspects (0); nearly or completely concealed by the *os spleniale* medially, that is, fenestra not visible in the medial aspect (1). The preserved (left) mandibular body of AMNH 3338 (fig. 11) shows a distinct mandibular fenestra (state 0).

**Character 104:** Mandible, articular, medial process (*os articulare, proc. medialis mandibulae*): not hooked (0); hooked (1). The process is curved rostromedially in all extant penguins. As Simpson (1946) noted, *Paraptenodytes* lacks a hooked process (fig. 10).

**Character 105:** Mandible, angular, retroarticular process (*mandibula, os angulare, proc. retroarticularis*), aspect in dorsal view in relation to the articular area with the quadrate (area between the lateral condyle [*condylus lateralis*] and medial condyle [*condylus medialis*]): broad, approximately equal to the articular area (0); moderately long, narrower

than the articular area (1); very long, longer and narrower than the articular area (2). *Paraptenodytes* exhibits a broad retroarticular process (state 0) that Simpson (1946) deemed similar to *Pygoscelis* (fig. 10). The outgroup taxa lack retroarticular process altogether (see character 106), and therefore were coded as noncomparable.

**Character 106:** Mandible, angular (*mandibula, os angulare*), aspect in dorsal view: sharply truncated caudally (0); caudally projected, forming the retroarticular process (*proc. retroarticularis*) (1). In *Paraptenodytes*, as in all penguins, the angular projects caudally, forming a retroarticular process (state 1), whose variation in shape was discussed in character 105 (fig. 10). This character supports the monophyly of Sphenisciformes.

**Character 107:** Mandible, caudal fossa (*mandibula, fossa caudalis*): shallow (0); deep (1). In *Paraptenodytes*, the caudal fossa of the mandible is shallow (state 0).

**Character 108:** Atlas (*atlas*), *proc. ventralis corporis*: absent or slightly developed (0); well developed, high with a prominent ridge (*crista ventralis corporis*) on the ventral surface of the *corpus atlantis* (1). *Paraptenodytes* clearly exhibits character state 1 (fig. 12) and shares it with *Aptenodytes* (and *Gavia* among the outgroup taxa), as noted by Simpson (1946).

**Character 120:** Coracoid, *foramen nervi supracoracoidei*: present (0), absent (1). This character was described by Mayr (2005), who discussed the homology of the conditions present in penguins and outgroup taxa. As in extant penguins, the foramen is absent in *Paraptenodytes* (fig. 16).

**Character 122:** Forelimbs (*ossa alae*), strongly flattened: absent (0); present (1). The humeri of AMNH 3338 are similar to those of other penguin forms, that is, strongly flattened (state 1; fig. 17).

**Character 123:** Humerus, aspect of pneumatic fossa (*humerus, fossa pneumotricipitalis*): small with pneumatic foramina (0); without pneumatic opening, moderate size (1); without pneumatic opening, great size and deep fossa (2). All penguin taxa, including *Paraptenodytes*, show a large pneumatic fossa without pneumatic opening (state 2; fig. 18).

**Character 124:** Humerus, head (*humerus, caput humeri*) large and reniform in shape,

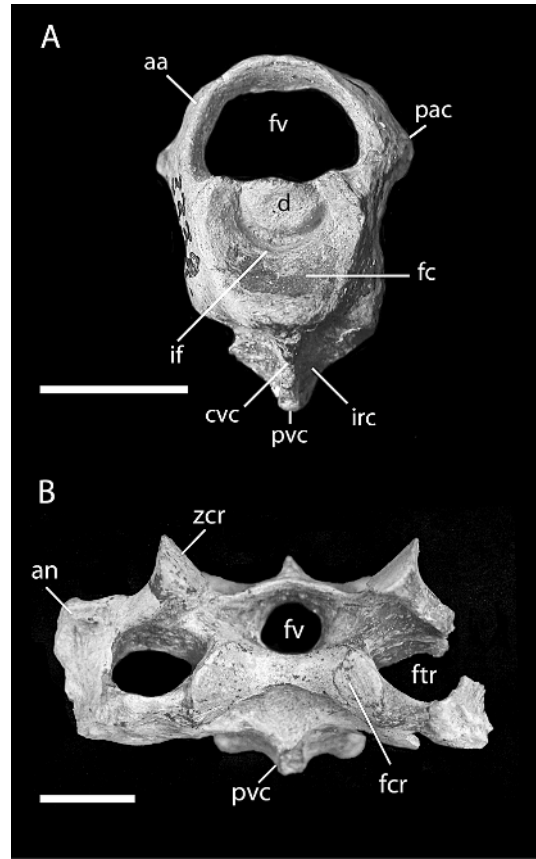


Fig. 12. Atlas (A) and 11th cervical vertebra (B) of *Paraptenodytes antarcticus* (AMNH 3338) in cranial aspect. Abbreviations: aa, arcus atlantis; an, ansa costotransversaria; cvc, crista ventralis corporis; dens axis; fc, fossa condyloidea; fcr, facies articularis cranialis; ftr, foramen transversarium; fv, foramen vertebrale; if, incisura fossae; pac, processus articularis caudalis; pvc, processus ventralis corporis; zcr, zygapophysis cranialis. Scale bars = 1 cm.

ventrally directed: absent (0); present (1). The shape of the humerus head in *Paraptenodytes* is typical of penguins (state 1, fig. 18).

**Character 125:** Humerus, pneumatic fossa (*humerus, fossa pneumotricipitalis*) subdivision into cavities: undivided (0); divided (1). In the previous analysis of this character, Bertelli and Giannini (2005) considered three states for the conditions observed in the pneumatic fossa—single, partially divided, and bipartite. The intermediate state was present only in

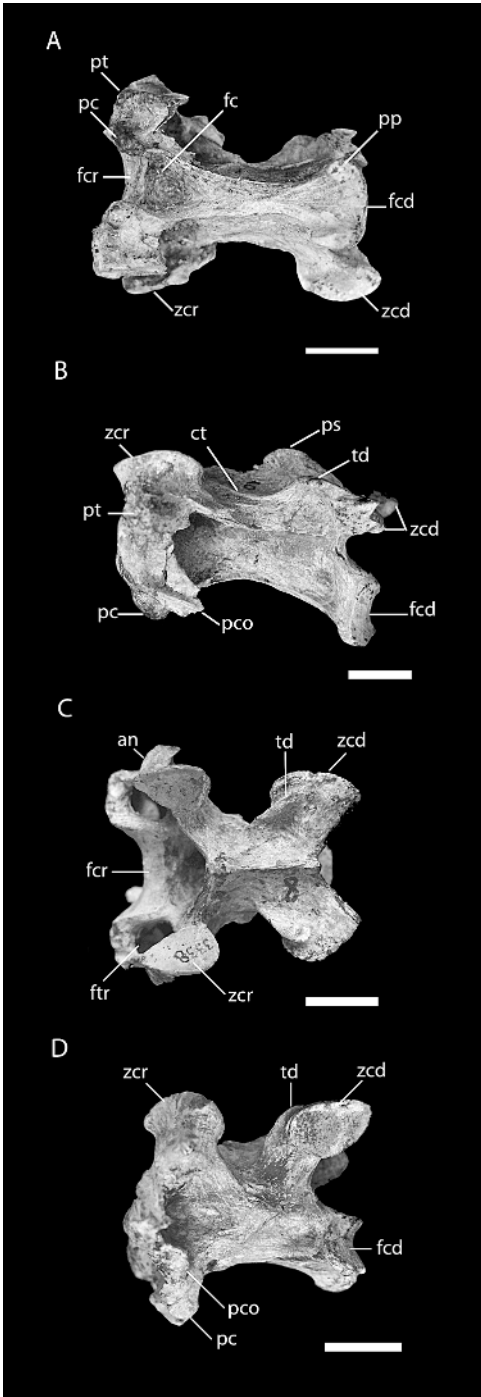


Fig. 13. Sixth cervical vertebra in ventral (A) and lateral (B) views; eighth cervical vertebra in dorsal (C) and lateral (D) view of *Paraptenodytes antarcticus* (AMNH 3338). Abbreviations: an, ansa

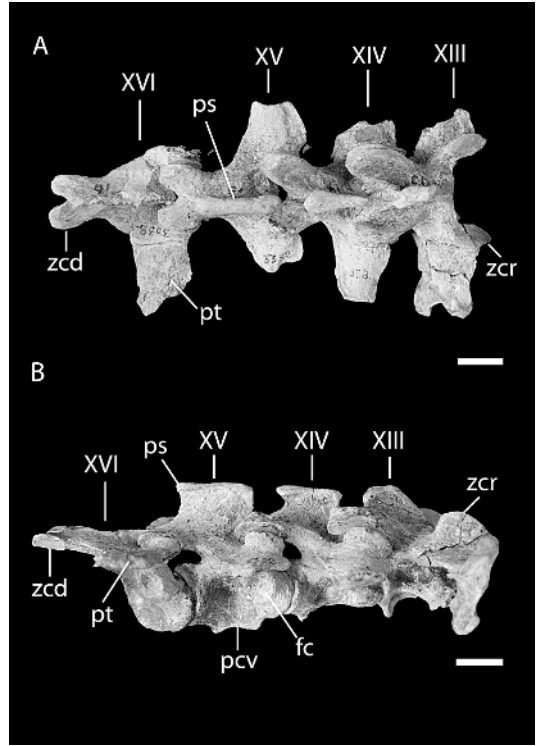


Fig. 14. Thirteenth to 16th vertebrae of *Paraptenodytes antarcticus* (AMNH 3338) in dorsal (A) and lateral (B) views. Abbreviations: XIII, 13th cervical vertebra; XIV, first thoracic vertebra; XV, second thoracic vertebra; XVI, thirteenth thoracic vertebra; fc, fovea costalis; ps, processus spinosus; pt, processus transversus; zcd, zygapophysis caudalis; zcr, zygapophysis cranialis. Scale bars = 1 cm.

*Eudyptula minor*. We reconsidered this coding and included just two states, the presence/absence of a divided pneumatic fossa. *Paraptenodytes*, as noted by Simpson (1946), lacks a distinct division of the pneumatic fossa in either the left or right humerus, and therefore it was scored 0 (fig. 18).

←

costotransversaria; ct, crista transverso-obliqua; fc, fovea cranioventralis; fcd, facies articularis caudalis; fcr, facies articularis cranialis; ftr, foramen transversarium; pc, processus caroticus; pco, processus costalis; pp, processus postlateralis; ps, processus spinosus; pt, processus transversus; td, torus dorsalis; zcd, zygapophysis caudalis; zcr, zygapophysis cranialis. Scale bars = 1 cm.

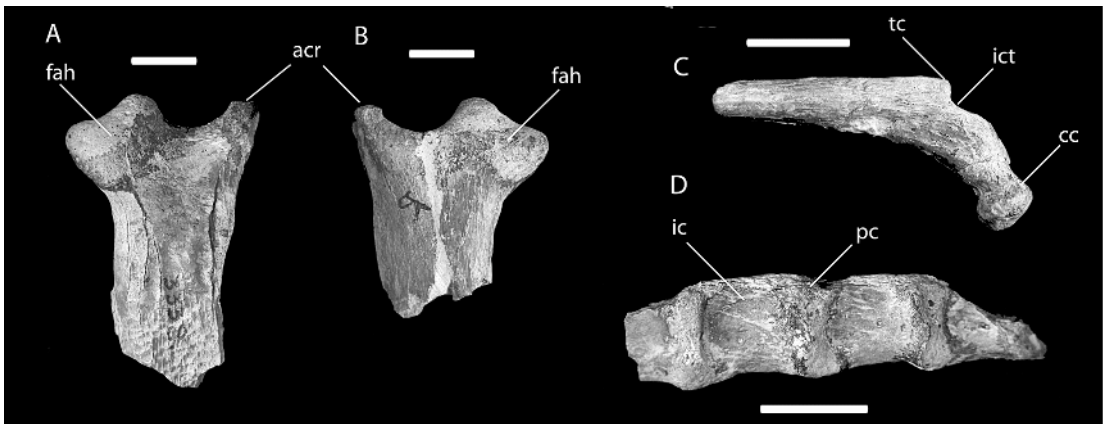


Fig. 15. Proximal ends of left (A) and right (B) scapulae, proximal end of a vertebral rib (C), and a right anterolateral fragment of sternum (D) of *Paraptenodytes antarcticus* (AMNH 3338). Abbreviations: acr: acromion; cc, capitulum costae; fah: facies articularis humeralis; ict, incisura capitulotubercularis; ic, incisura intercostalis; pc, processus costalis; tc, tuberculum costae. Scale bars = 1 cm.

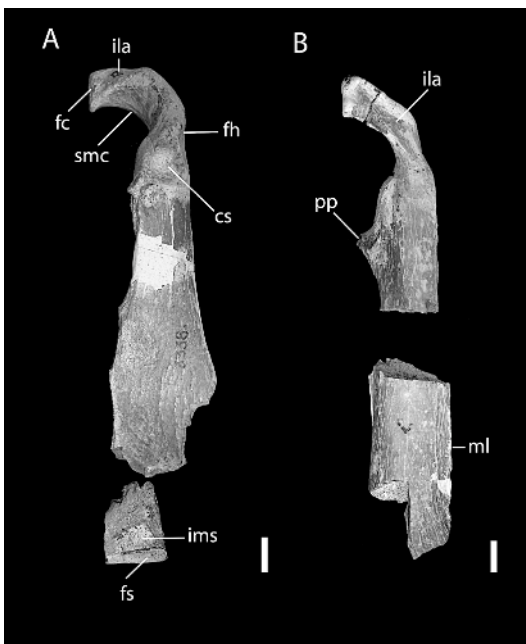


Fig. 16. Coracoideum of AMNH 3338, right in dorsal view (A) and left in ventral view (B). Abbreviations: cs, cotyla scapularis; fc, facies articularis clavicularis; fh, facies articularis humeralis; fs, facies articularis sternalis; ila, impressio lig. acrocoracohumeralis; ims, impressio *m. sternocoracoidei*; ml, margo lateralis; pp, processus procoracoideus; smc, sulcus *m. supracoracoidei*. Scale bars = 1 cm.

**Character 126:** Humerus, development of dorsal supracondylar process (*humerus, proc. supracondylaris dorsalis*): absent (0); compact tubercle (1); very long process (2). *Paraptenodytes* shares with all extant penguins the lack of supracondylar process (state 0; fig. 17).

**Character 127:** Humerus, deltoid crest, area of attachment of pectoral muscle (*humerus, crista deltopectoralis, impressio m. pectoralis*): shallow groove (0); deep, oblong fossa (1). The left and right humerus heads are preserved in AMNH 3338. As in extant penguins, the impression for the attachment of the pectoral muscle in *Paraptenodytes* is a deep fossa (state 1; fig. 17).

**Character 128:** Humerus, distal end, ventral border with “trochlear process” (caudalmost crest at the *epicondylus ventralis* caudally bordering the *sulcus humerotricipitalis*): present (0); absent (1). *Paraptenodytes* exhibits a trochlear process, a feature diagnostic of penguins (state 1; fig. 17).

**Character 129:** Humerus, proximalmost “trochlear process”: extends beyond the humeral shaft (0); does not extend beyond the humeral shaft (1). The proximal trochlear process does not extend beyond the humeral shaft in *Eudyptula* and *Spheniscus* (state 1) and in *Paraptenodytes*. In the remainder of extant genera, the proximal trochlear process does extend beyond the humeral shaft (state 0; fig. 17).



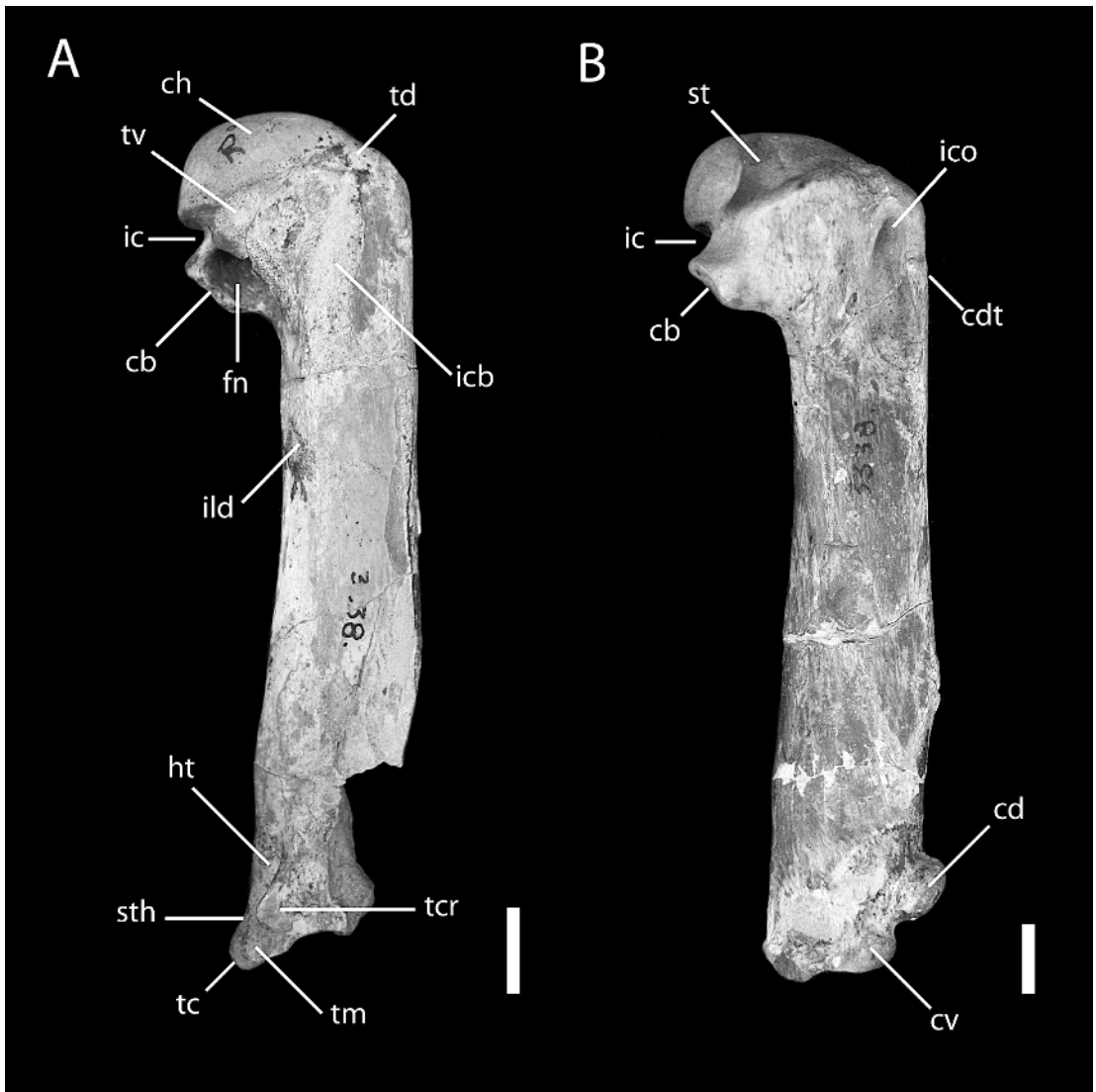


Fig. 17. Humerus of *Paraptenodytes antarcticus* (AMNH 3338), right side in cranial view (A) and left side in caudal view (B). Abbreviations: cb, crista bicipitalis; cd, condylus dorsalis; cdt, crista deltopectoralis; ch, caput humeri; cv, condylus ventralis; fn, fossa pneumotricipitalis; ht, sulcus humerotricipitalis; ic, incisura capitis; icb, impressio supracondylaris; ico, impressio coracobrachialis; st, sulcus lig. transversus; sth, sulcus scapulotricipitalis; tc, "caudal trochlear process"; tcr, "cranial trochlear process"; td, tuberculum dorsale; (cranialmost processlike crest at the epicondylus ventralis); tm, medial trochlear process; tv, tuberculum ventrale. Scale bars = 1 cm.

**Character 138:** Tarsometatarsus: slender, proximodistal length much greater than mediolateral width (0); very stout, mediolateral width nearly equal to proximodistal length (1). In AMNH 3338, the left and right tarsometatarsus are not complete. However, the pre-

served parts (fig. 21) permit a positive scoring of *Paraptenodytes*, which exhibits a typical spheniciform tarsometatarsus (state 1).

**Character 139:** Tarsometatarsus, blood vessel foramen located on *fossa para hypotarsalis medialis*: absent (0); present (1). Both the left

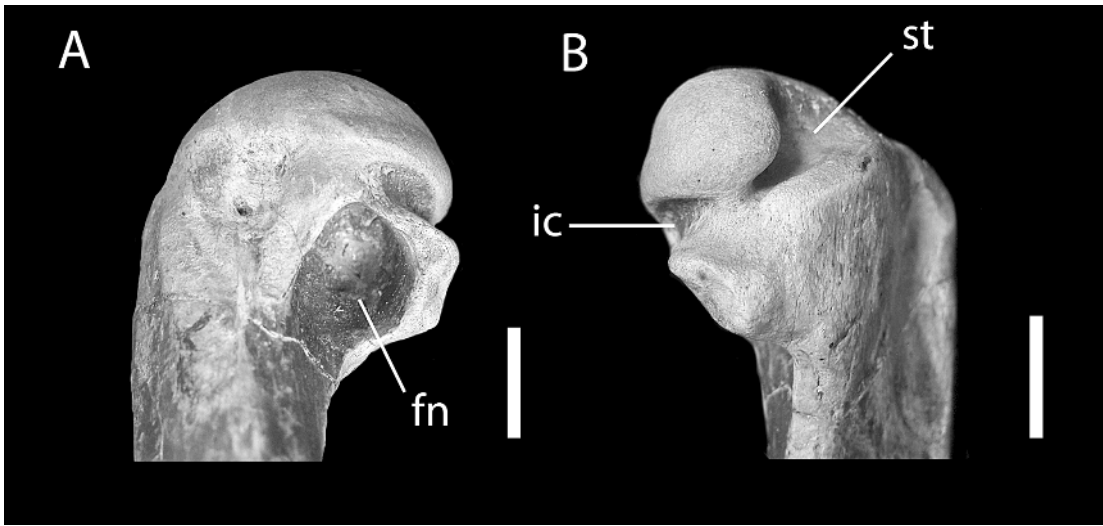


Fig. 18. Close-up of the proximal end of the right humerus of AMNH 3338 in caudal (A), and cranial (B) views. Abbreviations: ic, incisura capitis; st, sulcus lig. transversus; fn, fossa pneumotricipitalis. Scale bars = 1 cm.

and right tarsometatarsus of AMNH 3338 lack this vascular foramen (state 0; fig. 21).

**Character 140:** Tarsometatarsus, medial proximal vascular foramen (*foramina vascularia proximalia*): absent (0); present (1). The proximal foramen opens lateral to medial crest (*crista medialis hypotarsi*). The left and right tarsometatarsus of AMNH 3338 exhibit this foramen visible in the plantar side (state 1; fig. 21).

**Character 141:** Tarsometatarsus, hypotarsus, tendinal canals (*hypotarsus, canales hypotarsi*): present (0); absent (1). All penguins, including *Paraptenodytes*, lack tendinal canals in the proximal end of the tarsometatarsus (state 1; fig. 21).

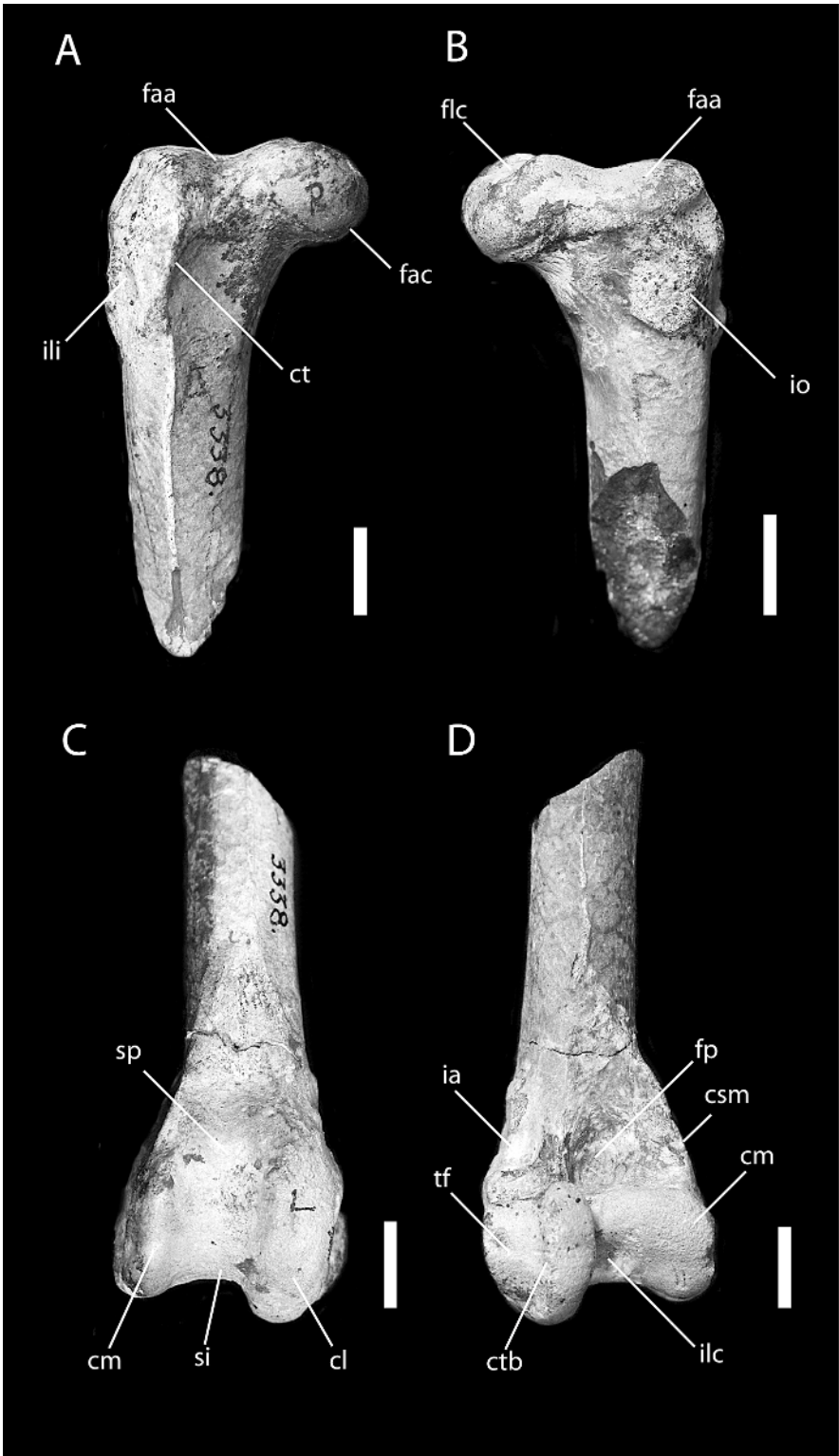
**Character 142:** Tarsometatarsus, *tuberositas m. tibialis cranialis*: flat (0); raised (1). A raised *tuberositas tibialis* is present in all penguins

(state 1) except *Aptenodytes* (state 0). AMNH 3338 shows a raised tubercle in both the left and right tarsometatarsus (fig. 21).

#### TOPOLOGIES

The analysis including only the osteological characters initially resulted in 425 most parsimonious trees; an extra TBR round on optimal trees elevated this number to a total of 2004 equally optimal trees at 148 steps (strict consensus in fig. 22) The consensus recovered Procellariiformes (unresolved) and Sphenisciformes, but overall resolution and support was poor. Absolute Bremer support values (hereafter ABS) were low, as ABS = 2 in all resolved nodes (calculated on the basis of a sample of 16,000 suboptimal trees). *Paraptenodytes antarcticus* was the sister to

Fig. 19. Femur of *Paraptenodytes antarcticus* (AMNH 3338), proximal end of the right side in cranial (A) and caudal (B) aspects; distal end of the left side in cranial (C) and caudal (D) aspects. Abbreviations: cl, condylus lateralis; cm, condylus medialis; csm, crista supracondylaris medialis; ct, crista trochanteris; ctb, crista tibiofibularis; faa, fascies articularis antitrochanterica; fac, facies articularis acetabularis; flc, fovea lig. capitis; fp, fossa poplitea; ia, impressio anae m. iliofibularis; ilc, impressio lig. cruciati cranialis; ili, impressioes iliiochantericae; io, impressioes obturatoriae; si, sulcus intercondylaris; sp, sulcus patellaris; tf, trochlea fibularis. Scale bars = 1 cm.



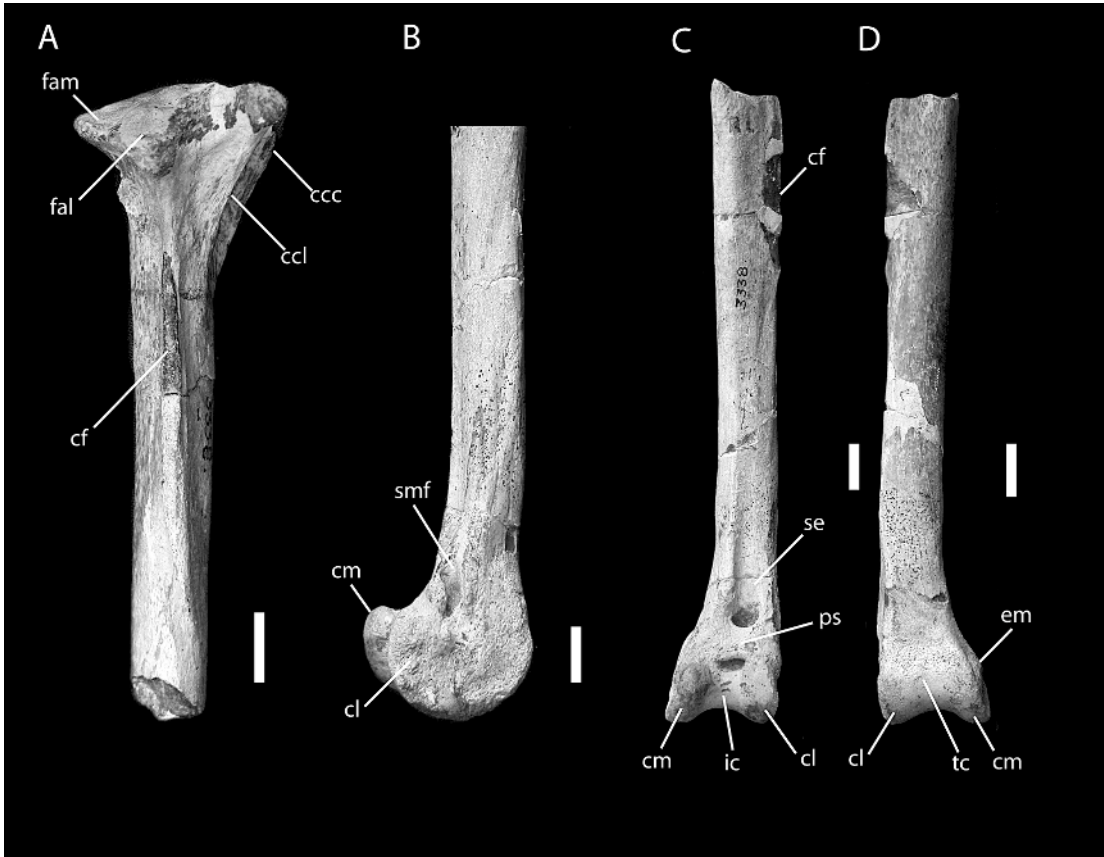


Fig. 20. Proximal end of right tibiotarsus of *Paraptenodytes antarcticus* (AMNH 3338) in craniolateral aspect (A); close-up of left tibiotarsus, lateral aspect (B); left tibiotarsus in cranial (C) and caudal (D) aspects. Abbreviations: ccc, crista cnemialis cranialis; ccl, crista cnemialis lateralis; cf, crista fibularis; cl, condylus lateralis; cm, condylus medialis; em, epicondylus medialis; fal, facies articularis lateralis; fam, facies articularis medialis; ic, incisura intercondylaris; ps, pons supratendineus; se, sulcus extensorius; smf, sulcus *m. fibularis*; tc, trochlea cartilaginis tibialis. Scale bars = 1 cm.

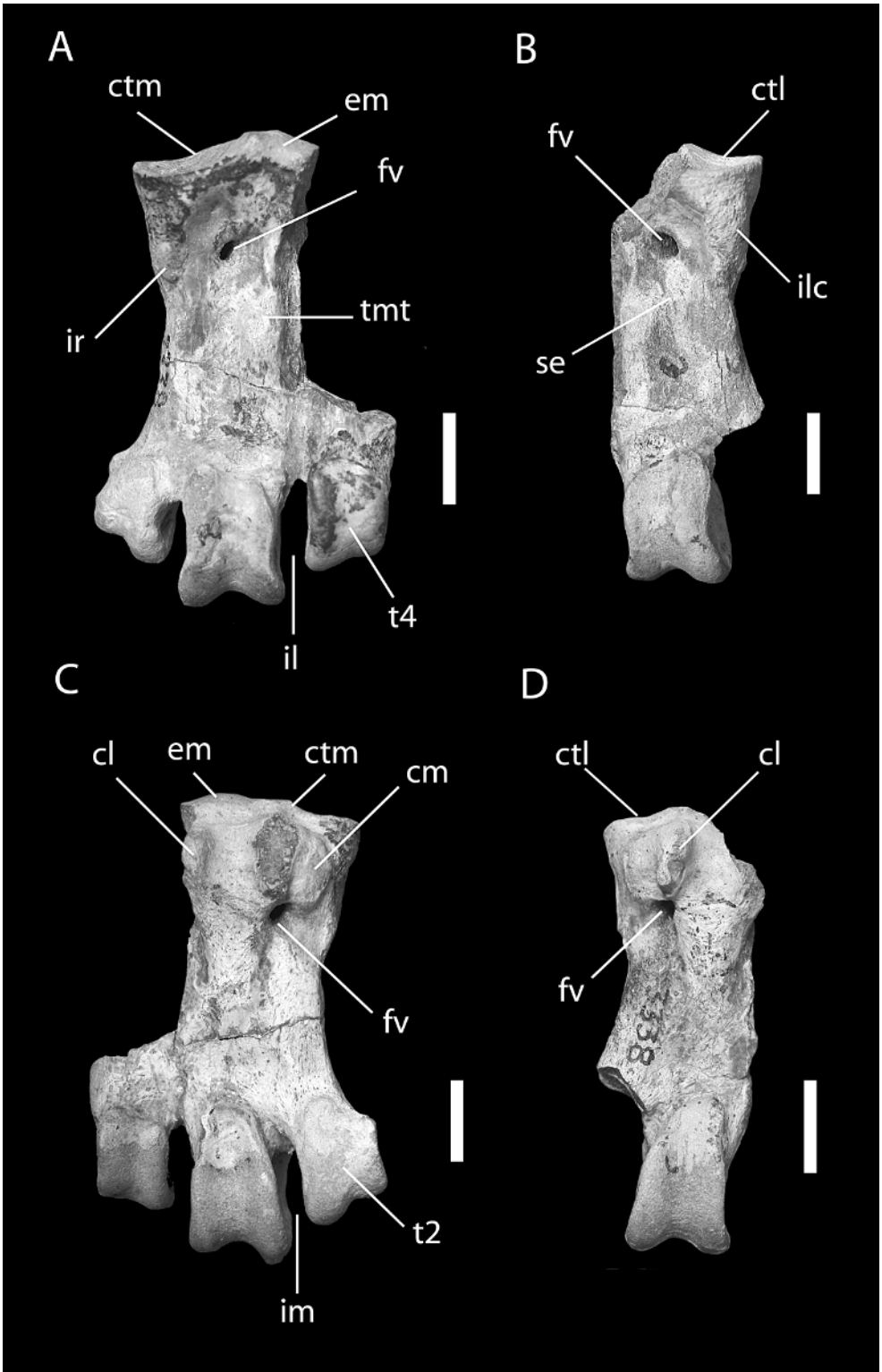
all extant penguins. *Eudyptula*, a monophyletic *Spheniscus*, and a clade containing the remaining genera formed a trichotomy. Within the last group, two clades appeared, one including *Pygoscelis papua*, a clade containing the other two species of *Pygoscelis*, and *Aptenodytes*, and another clade formed by *Megadyptes* and

*Eudyptes*. Relationships within the polytypic genera were unresolved.

The analysis including all nonmolecular characters (morphological and behavioral traits) yielded two optimal trees of 393 steps (strict consensus in fig. 23). The tree was almost fully resolved, the consensus showing

→

Fig. 21. Tarsometatarsus of *Paraptenodytes antarcticus*; left (A) and right (B) side in dorsal aspect; left (C) and right (D) side in plantar aspect. Abbreviations: cl, crista lateralis hypotarsi; cm, crista medialis hypotarsi; ctl, cotyla lateralis; ctm, cotyla medialis; em, eminentia intercotylaris; fv, foramina vascularia proximalia; il, incisura intertrochlearis lateralis; ilc, impressio lig. collateralis lateralis; im, incisura intertrochlearis medialis; ir, impressio retinaculi extensorii; se, sulcus extensorius; tmt, tuberositas *m. tibialis cranialis*; t2, trochlea metatarsi II; t4, trochlea metatarsi IV. Scale bars = 1 cm.



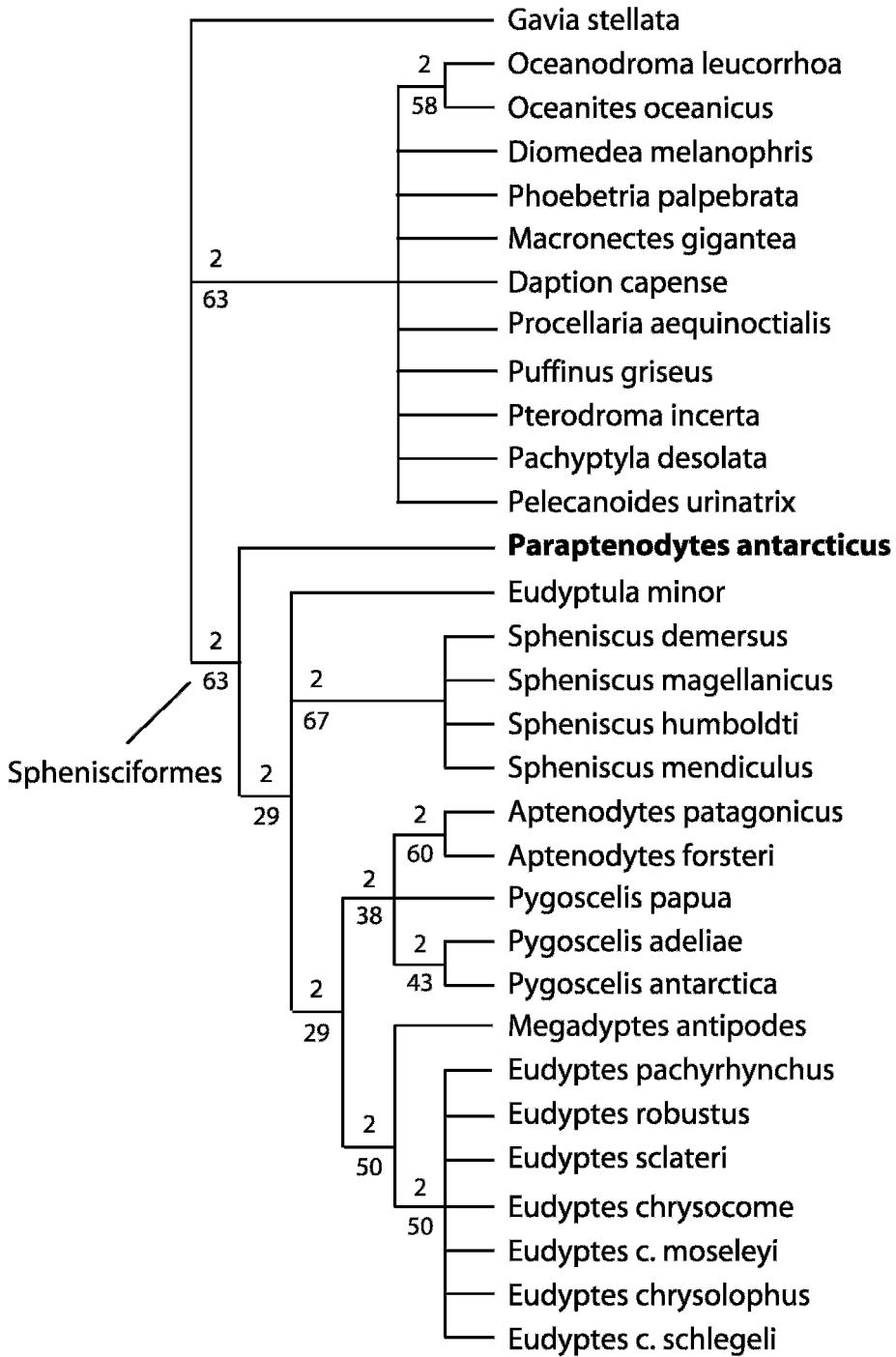


Fig. 22. Strict consensus tree from 2004 trees of 148 steps, osteological dataset. Absolute Bremer values are above branches, relative values are below branches. Bremer values were calculated from a sample of 16,000 trees (see Methods). CI = 0.60, RI = 0.90.

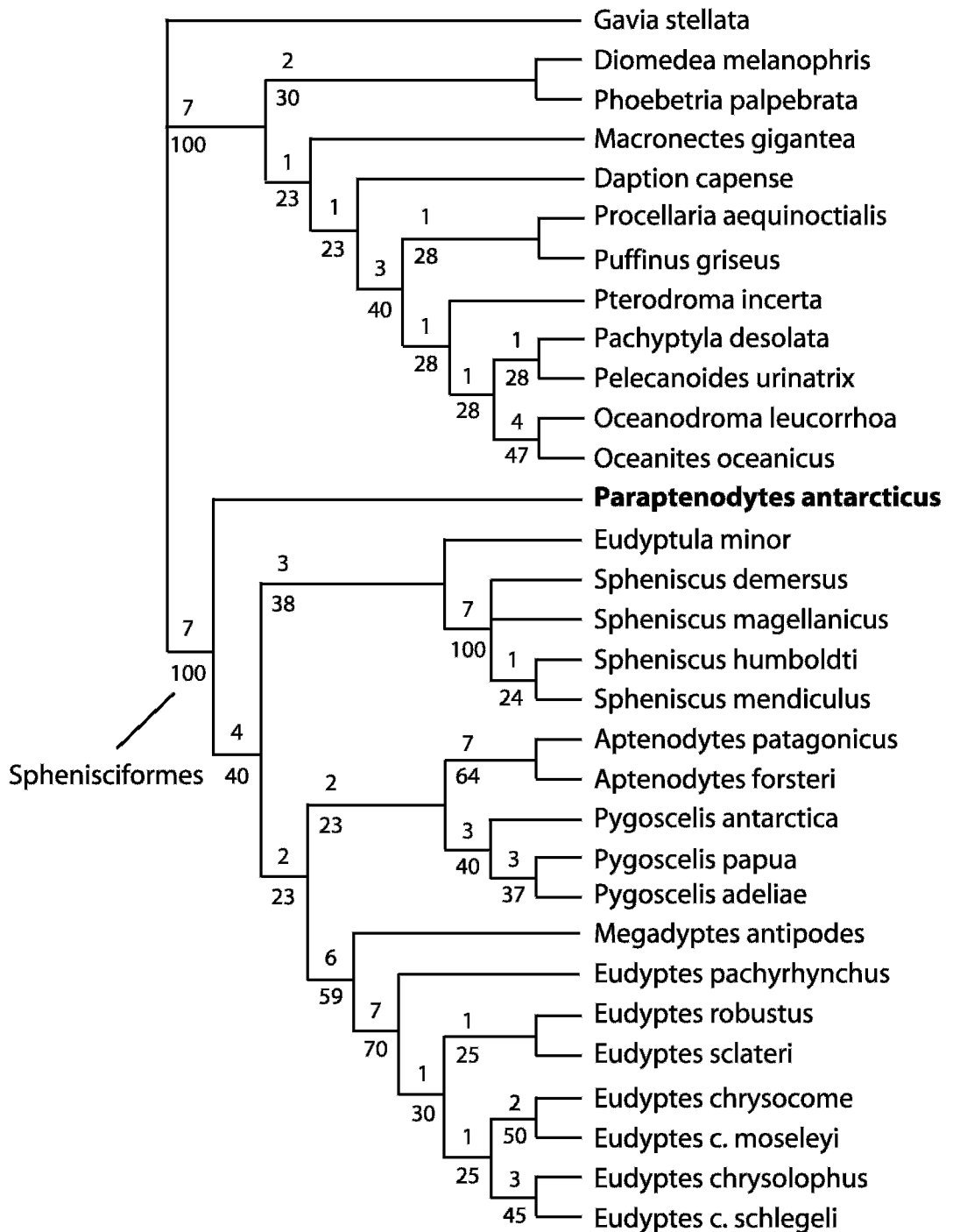


Fig. 23. Strict consensus tree from two trees of 393 steps, total morphological dataset (osteology, soft tissue, behavior, and oology). Absolute Bremer values are above branches, relative values are below branches. Bremer values were calculated from a sample of 10,520 trees (see Methods). CI = 0.62, RI = 0.86.

just a trichotomy within *Spheniscus*. Within procellariiforms, albatrosses formed a clade sister to all other procellariiforms. In the latter clade, the successive sister groups were *Macronectes*, *Daption*, and a clade formed by shearwaters (*Procellaria* + *Puffinus*), *Pterodroma*, and a group composed of an oceanitid clade (*Oceanites* + *Oceanodroma*) and a composite clade including the prion *Pachyptila* and the diving petrel *Pelecanoides*. In the penguin subtree, *Paraptenodytes* was the sister of all extant forms, Spheniscidae (sensu Clarke et al., 2003). The topology within Spheniscidae is the same as that recovered by the morphological analysis of Bertelli and Giannini (2005). *Eudyptula* + *Spheniscus* form the sister group to a clade containing the remainder of the genera. The latter clade is split into two groups, one including *Aptenodytes* and *Pygoscelis*, the other including *Megadyptes* and *Eudyptes*. In *Spheniscus*, the Pacific forms *S. humboldti* and *S. mendiculus* grouped together. Within *Pygoscelis*, *P. antarctica* was sister to the other two species. *Eudyptes pachyrrhynchus* was sister to the other congeners, and successive sister groups were (*E. robustus* + *E. sclateri*), (*E. chrysocome chrysocome* + *E. chrysocome moseleyi*), and (*E. chrysolophus* + *E. schlegeli*). ABS values, calculated from a sample of 10,520 suboptimal trees up to seven steps longer than the optimals, were higher for recovered genera ( $3 \leq \text{ABS} \leq 7$ ) and for orders (ABS for Procellariiformes and Sphenisciformes = 7). Relative Bremer support values (RBS) followed a pattern similar to absolute Bremer values; that is, backbone nodes exhibited the highest conflict (RBS as low as 23), recovered genera (RBS  $\geq 40$ ) and Sphenisciformes (RBS as high as 100) the lowest conflict.

The combined analysis (molecular + non-molecular data) yielded two trees of 2329 steps (strict consensus in fig. 24). Procellariiformes and Sphenisciformes were monophyletic. The former clade was fully resolved; the successive sister clades recovered were Oceanitidae, Diomedidae, (*Pterodroma* + *Puffinus*), (*Pachyptila* + *Pelecanoides*), *Procellaria*, and the fulmarine petrels (*Daption* + *Macronectes*). Support values were moderate to high ( $4 \leq \text{ABS} \leq 17$ ), except for the sister group to

Oceanitidae (ABS = 1). The penguin subtree was fully resolved except for a trichotomy in *Spheniscus*. *Paraptenodytes* appeared as sister to all extant forms. Successive sister groups within the crown group of extant penguins were *Aptenodytes*, *Pygoscelis*, and clade E of Bertelli and Giannini (2005), composed of (*Eudyptula* + *Spheniscus*) and (*Megadyptes* + *Eudyptes*). Intrageneric relationships were as follows. Within *Pygoscelis*, unlike the nonmolecular analysis, *P. adeliae* was sister to the other two species. Relationships remained unchanged within *Spheniscus* and *Eudyptes* with respect to the nonmolecular analysis. Lowest support values occurred within *Eudyptes* ( $1 \leq \text{ABS} \leq 3$ ). The backbone of the penguin subtree was moderately supported ( $4 \leq \text{ABS} \leq 5$ ), taking into account the fact that this arrangement of suprageneric groups strongly contradicts the nonmolecular analysis. The conflict between the two trees reflects the differential rooting of the same basic network favored by the molecular (on *Aptenodytes*) and nonmolecular (on *Eudyptula* + *Spheniscus*) partitions, as discussed by Bertelli and Giannini (2005). All genera were recovered and well supported ( $6 \leq \text{ABS} \leq 8$ ).

## DISCUSSION

*Paraptenodytes antarcticus* was placed in a subfamily of its own by Simpson (1946; Paraptenodytinae), separate from all living forms. This hypothesis of relationships was supported by our analyses, given that *Paraptenodytes* appeared as sister taxon to a clade containing all extant genera. The inclusion of *Paraptenodytes* in morphological and combined analyses did not change the perceived relationships within Sphenisciformes from previous analyses (Bertelli and Giannini, 2005). Neither the topology nor the support values of the penguin tree were seriously affected by the inclusion of this fossil. Furthermore, the topology of the extant clade is very similar (except for some clades within *Eudyptes*) to the one recovered by Baker et al. (2006) using nuclear and mitochondrial genes. These facts together contribute to a stable view of the relationships of extant penguins.



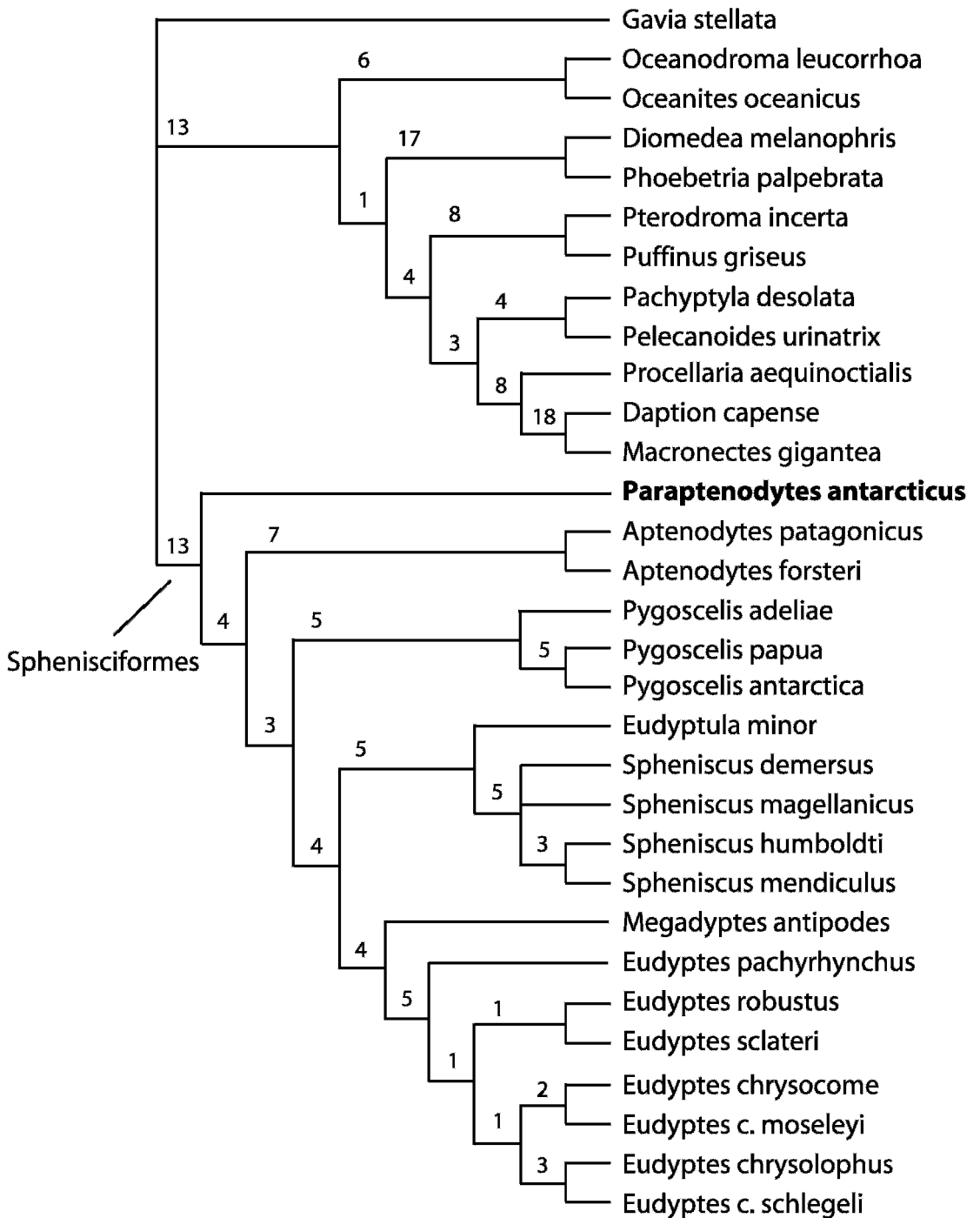


Fig. 24. Strict consensus tree from two trees of 2329 steps, total morphological + molecular dataset. Bremer values appear above branches.

*P. antarcticus* shares numerous synapomorphies with Spheniscidae, thereby reinforcing its well-established status as a typical stem penguin. This taxon also retains several plesiomorphic traits, both in the skull and the postcranium, whose alternative character states optimized as synapomorphies of extant penguins. Primitive features retained by *P. antarcticus* include a deep subcondylar fossa on the basioccipital (character : state 1), an elongated, unexpanded pterygoid (89:0), an unhooked medial process of the articular (104:0), and an undivided fossa pneumotricipitalis (125:0). *P. antarcticus* also possesses numerous autapomorphic features, including a distinctly bifid paraoccipital process, and dorsally extended temporal fossae that end squarely in the sagittal plane (Simpson, 1946).

Simpson (1972) included two other species in the genus *Paraptenodytes*: *P. robustus* and *P. brodkorbi*. He provided the following diagnosis for the genus: humerus moderately elongate; shaft nearly straight and slightly narrower proximally; preaxial angle slight, distal and rounded; tricripital fossa deep and not bipartite; tarsometatarsus short and stout (ratio of length to proximal width approximately 2 or less); metatarsals strongly fused with two small, proximal intermetatarsal foramina. We examined a cast of the holotype of *P. robustus* (BMNH A591) and figures of *P. brodkorbi* (Ameghino, 1905: pl. 5, fig. 29a+e) in this study. The humerus of *P. robustus* is shorter and wider than that of *P. antarcticus*, but is otherwise similar to *P. antarcticus*, particularly in the straightness of the shaft. This species also possesses an undivided tricripital fossa and a large shelf adjacent to the ulnar condyle, but both features are seen in all Paleogene fossil penguins and almost certainly primitive for the clade. *P. brodkorbi*, however, shows marked differences from *P. antarcticus* and *P. robustus*, including a more angled shaft and a more well-developed preaxial angle. Therefore, *P. brodkorbi* lacks the most diagnostic characters of *Paraptenodytes* and probably belongs outside the genus. A rigorous test of the monophyly of the genus requires an expanded sampling of fossil taxa and characters and is beyond the scope of this paper.

## CONCLUSIONS

The skull of *Paraptenodytes antarcticus* displays many unique features compared to extant penguins. Cladistic analyses incorporating all extant penguins and *P. antarcticus* place this taxon as the sister taxon to a clade including all living forms (Spheniscidae). Examining *P. antarcticus* in a phylogenetic framework reveals the order of acquisition of many penguin synapomorphies. The placement of this South American fossil as sister taxon to the Spheniscidae highlights the possibility of a Subantarctic, rather than Antarctic, origin of extant penguins. As the relationships of other fossil taxa are resolved, we will be better able to incorporate fossil data into biogeographical analyses. Although we were unable to include all named species of *Paraptenodytes* in our analysis, we strongly suspect the genus is nonmonophyletic. The inclusion of additional taxa in future analyses will enable finer resolution of the phylogenetic position of *P. antarcticus* relative to other fossil penguins and provide a basis for revision of the genus *Paraptenodytes*.

## ACKNOWLEDGMENTS

For permitting access to materials, we thank C. Mehling (Department of Vertebrate Paleontology) and P. Sweet (Department of Ornithology) of the American Museum of Natural History (New York, USA); P. A. Tubaro (Museo Argentino de Ciencias Naturales, Buenos Aires, Argentina); E. Alabarce (Coleccion Ornitologica Lillo, Tucuman, Argentina); M. Adams (Bird Division) and S. Chapman (Palaeontology Department) of The Natural History Museum (UK); D. Willard, J. Bates, and S. Hackett (Field Museum of Natural History, Chicago, USA); and K. Garrett (Natural History Museum of Los Angeles County, Los Angeles, USA). S. Bertelli thanks the Chapman Memorial Fund at the AMNH and the Antorchas Foundation at the LACM for postdoctoral support. N. Giannini thanks the Vernay Postdoctoral Fellowship at the AMNH. Reviews by Estelle Bourdon and Tim Crowe significantly improved this article.

## REFERENCES

- Acosta Hospitaleche, C., and J. Canto. 2005. Primer registro de cráneos asignados a *Palaeospheniscus* (Aves, Spheniscidae) procedentes de la Formación Bahía Inglesa (Mioceno Medio-Tardío), Chile. *Revista Chilena de Historia Natural* 78: 489–495.
- Ameghino, F. 1905. Enumeracion de los impennes fosiles de Patagonia y de la Isla Seymour. *Anales del Museum Nacional de Buenos Aires* (series 3) 6: 97–167.
- Baker, A.J., S.L. Pereira, O.P. Haddrath, and K.-A. Edge. 2006. Multiple gene evidence for expansion of extant penguins out of Antarctica due to global cooling. *Proceedings of the Royal Society, B* 217: 11–17.
- Baumel, J.J., A.S. King, J.E. Breazile, H.E. Evans, and J.C. Vanden Berge (editors). 1993. *Handbook of avian anatomy: nomina anatomica avium*, 2<sup>nd</sup> ed. Publications of the Nuttall Ornithological Club 23: 1–779.
- Bertelli, S., and N.P. Giannini. 2005. Phylogeny of extant penguins (Aves: Sphenisciformes) combining morphology and mitochondrial sequences. *Cladistics* 21: 209–239.
- Bock, W.J. 1960. Secondary articulation of the avian mandible. *Auk* 77: 130–132.
- Brodkorb, P. 1963. Catalogue of fossil birds, part 1 (Archaeopterygiformes through Ardeiformes). *Bulletin of the Florida State Museum* 7: 179–293.
- Clarke, J.A., E.B. Olivero, and P. Puerta. 2003. Description of the earliest fossil penguin from South America and first paleogene vertebrate locality of Tierra del Fuego, Argentina. *American Museum Novitates* 3423: 1–18.
- Elzanowski, A. 1987. Cranial and eyelid muscles and ligaments of the tinamous (Aves: Tinamiformes). *Zoologische Jahrbuecher Abteilung fuer Anatomie und Ontogenie der Tiere* 116(1): 63–118.
- Elzanowski, A., G.S. Paul, and T.A. Stidham. 2000. An avian quadrate from the late Cretaceous Lance Formation of Wyoming. *Journal of Vertebrate Paleontology* 20: 712–719.
- Fuchs, A. 1954. On the correlation between the skull structure and the muscles in the male *Phasianus colchicus* L. IV. The attachment of the musculus protractor quadrati et pterygoidei and of the musculus depressor mandibulae. *Koninkilge Nederlandse Akademie van Wetenschappen, Proceedings, C* 57: 666–672.
- Giannini, N.P., and S. Bertelli. 2004. Phylogeny of extant penguins based on integumentary and breeding characters. *Auk* 121: 422–434.
- Giannini, N.P., and N.B. Simmons. 2003. A phylogeny of megachiropteran bats (Mammalia: Chiroptera: Pteropodidae) based on direct optimization analysis of one nuclear and four mitochondrial genes. *Cladistics* 19: 496–511.
- Goloboff, P.A. 1999. Analyzing large data sets in reasonable times: solutions for composite optima. *Cladistics* 15: 415–428.
- Goloboff, P.A., J.S. Farris, and K. Nixon. 2004. T.N.T. : Tree analysis using new technologies. Program and documentation, available at [www.cladistics.org](http://www.cladistics.org).
- Hofer, H. 1950. Zür morphologie der kiefermuskulatur der Vogel. *Zoologische Jahrbuecher Abteilung fuer Anatomie und Ontogenie der Tiere* 70: 427–600.
- Ksepka, D.T., and S. Bertelli. In press. Fossil penguin (Aves: Sphenisciformes) cranial material from the Eocene of Seymour Island (Antarctica).
- Marples, B.J. 1962. Observations on the history of penguins. In G.W. Leeper (editor), *The evolution of living organisms: 408–416*, Melbourne University Press: Melbourne.
- Mayr, G. 2005. Tertiary plotopterids (Aves, Plotopteridae) and a novel hypothesis on the phylogenetic relationships of penguins (Spheniscidae). *Journal of Zoological and Systematic Evolutionary Research* 43: 61–71.
- Moreno, F.P., and A. Mercerat. 1891. *Paleontologia Argentina I. Catalogo de los Pajaros de la Republica Argentina Conservados en el Museo de la Plata*.
- Nixon, K.C. 1999. The parsimony ratchet, a new method for rapid parsimony analysis. *Cladistics* 15: 407–414.
- Pycraft, W.P. 1898. Contribution to the osteology of birds. Part II. Impennes. *Proceedings Zoological Society of London* 1898: 958–989.
- Saiff, E.I. 1976. Anatomy of the middle ear region of the avian skull: Sphenisciformes. *Auk* 93: 749–759.
- Schreiwies, D.O. 1982. A comparative study of the appendicular musculature of penguins (Aves: Sphenisciformes). *Smithsonian Contributions in Zoology* 341: 1–46.
- Simpson, G.G. 1946. Fossil penguins. *Bulletin American Museum of Natural History* 87: 1–100.
- Simpson, G.G. 1972. Conspectus of Patagonian fossil penguins. *American Museum Novitates* 2488: 1–37.
- Simpson, G.G. 1976. Fossil penguins. In B. Stonehouse (editor), *The biology of the penguins: 19–41*. London: Macmillan Press Ltd.
- Slack, K.E., C.M. Jones, T. Ando, G.L. Harrison, R.E. Fordyce, U. Arnason, and D. Penny. 2006. Early penguin fossils, plus mitochondrial genome calibrate avian evolution. *Molecular Biology and Evolution*. 10.1093/molbev/msj124.

- Stucchi, M. 2002. Una nueva especie de *Spheniscus* (Aves: Spheniscidae) de la Formacion Pisco, Peru. Boletin de la Sociedad Geologica del Peru 94: 17–24.
- Stucchi, M., M. Urbina, and A. Giraldo. 2003. Una nueva especie de Spheniscidae del Mioceno Tardio de la Formacion Pisco, Peru. Bulletin de l'Institut Francais d'Etudes Andines 32(2): 361–376.
- Watson, M. 1883. Report on the anatomy of the Spheniscidae collected during the voyages of H.M.S. Challenger. In J. Murray (editor), Report on the scientific results of the voyage of H.M.S. Challenger during the years 1873–

1876, Zoology, Vol. 7: 1–244. Edinburgh: Neill and Company.

- Wheeler, W.C. 1996. Optimization alignment: the end of multiple sequence alignment in phylogenetics? Cladistics 12: 1–9.
- Wheeler, W.C. 2003. Iterative pass optimization of sequence data. Cladistics 19: 254–260.
- Wheeler, W.C., D.S. Gladstein, and J. De Laet. 2003. POY. Version 3.0.11. ftp.amnh.org/pub/molecular/poy.
- Zusi, R.L. 1975. An interpretation of skull structure in penguins. In B. Stonehouse (editor), The biology of penguins, 59–84. Baltimore: University Park Press.

## APPENDIX 1

### LIST OF SPECIMENS EXAMINED

Abbreviations of Institutions: **AMNH**, American Museum of Natural History, New York, USA; **BMNH**, Natural History Museum, Tring, UK; **COL**, Coleccion Ornitológica Lillo, Facultad de Ciencias Naturales e IML, Tucumán, Argentina; **FMNH**, Field Museum of Natural History, Chicago, USA; **LACM**, Natural History Museum of Los Angeles County, Los Angeles, USA; **MACN**, Museo Argentino de Ciencias Naturales “Bernardino Rivadavia”, Buenos Aires, Argentina. Taxa are listed alphabetically.

1. Integumentary specimens: *Aptenodytes forsteri* AMNH 196281–2, 265389, 435602–7, 435609–11, 435613–4, 525862, 525867–71, 793545, LACM 69986; *Aptenodytes patagonicus* AMNH 132452–3, 132456, 132459, 132460–1, 269635, 428536, 435830, 435832, 443456, 442457, 525873–7, 525879–84, 525886, 525888–9, COL 10988; *Daption capense* AMNH 445493–4, COL 8089–93, 8095; *Eudyptes chrysocome chrysocome* AMNH 196414, 211923, 211991–2, 211994, 211996–7, 211999, 212002, 212009, 215732, 215759, 445213–20, 445222–6, 525731, 525733, 525736, 525738, 525740, 525743, 525745–52, 525754–8, 525760, 525762–3, 525765–73, COL 10986, 582–263; *Eudyptes chrysolophus* AMNH 196167–71, 349606, 445227–8, 5257926, BMNH 1905.12.30.164 [holotype], COL 10987; *Eudyptes pachyrrhynchus* AMNH 29898, 525703–4, 525707–8, 525713, 525726, BMNH 1845.1.13.29 [holotype]; *Eudyptes schlegeli* AMNH 211984, 525798–810, 525812; *Eudyptes sclateri* AMNH 196413, 212001, 212003–5, 212007, 212010–1, 525714, 525722, 525777, 525780–5, 525787, 525789, 525791, BMNH 1889.4.7.1 [holotype]; *Eudyptes robustus* AMNH 525720–1, 525723, 748427; *Eudyptula minor albosignata* AMNH 212016, 212018–9, 212021–5, 220909, 225701, 525702; *Eudyptula minor minor* AMNH 168804, 220910, 212013–15, 525528, 525599–603, 525605–

21, 525623–4, 525627, 525629–30, 5256324, 525636–7, 525651, 525685, LACM 23909–11; *Diomedea melanophrys* AMNH 445399, 445410, 445417–8, 445420, COL 5936–9, 598–2729; *Gavia stellata* AMNH 525949, 525951, 525987, 703321, BMNH 1935.9.9.36, 1937.10.17.157, 1937.10.17.158, 1965.m.134; *Macronectes giganteus* AMNH 211703, 749313, COL 600, 5940–1; *Megadyptes antipodes* AMNH 461127–8, 525843–59, 525861–2, 5258646, LACM 101235; *Oceanites oceanicus* COL 8121, 8123, 8125–9; *Oceanodroma leucorhoa* AMNH 70249, 70252, 79397, 349391, 528706; *Pachyptila desolata* AMNH 132519, 269679, 269682, 269285, 407676, COL 12831; *Pelecanoides urinatrix* AMNH 212088, 334637, 528738, 528760, 748433, COL 12445; *Phoebastria palpeb-rata* AMNH 26714, 132538, 196430, 211408, 527084, 749332, COL 10992; *Procellaria aequinoctialis* AMNH 211612, 211616, 527317, COL 10095–6; *Pterodroma incerta* AMNH 132491–2, 269656, 269659, 527987; *Puffinus griseus* AMNH 211986–7, 748419, 749268, 527606, COL4219,5893–7; *Pygoscelis adeliae* AMNH 196161–3, 325834, 325245, 325247–9, 435615–6, 442407–8, 442410–1, 525833, 525835–9, LACM 54430, 63897, COL 8138; *Pygoscelis antarctica* AMNH 196159, 132460, 168780,168806, 190158, 196156, 196160, 349607, 442419–21, 525840–2, 775711, COL 8136; *Pygoscelis papua* AMNH 132462–9, 196165–6, 196415, 269638–9, 435821–9, 442412–7, 442458–62, 445204–12, 525819–20, 525822, 525824–31, 775712, COL 8019, 8137, 14043, 15837–9, two specimens uncataloged; *Spheniscus demersus* AMNH 139880, 300427, 525902–3, 525905, 525908–11, 525913–6, BM 1911.12.18.13, 1939.5.11.1, 1939.5.11.2, 1987.2.4.191, 1987.24.211, 1987.24.212, LACM 20531; *Spheniscus humboldti* AMNH 147869, 196395, 305680, 305682–5, 308767, 357489, 44522931, 525937, 828554, BM 1913.10.11.112, LACM 18007, 18473, 18498, 25439–40, 50001–2, 84448, COL uncataloged; *Spheniscus magellanicus* AMNH 445240–1, 525890, LACM 25436–8, 69988, COL 4206, 7217, 7235–8, 12378, 16001, 581–2642, two specimens

uncataloged; *Spheniscus mendiculus* AMNH 178170, 196305–6, 266348, 292163, 292233–4, 292636, 299219, 407655, 442424, 525917, 525919–34, 525936, 804313–5, LACM 18649, 18653, 20056, 30295–8, 35882, 84451.

2. Osteological specimens: *Aptenodytes forsteri* AMNH 3745, 3725, 3727, 3767, 4856, 8110–2, 11634, 12002, FMNH 106829, 339515, LACM 99854, USNM 346249, 346257, 488188, 553580, 555520; *Aptenodytes patagonicus* AMNH 83, 2611, 4382, 26471–2, FMNH 351211, 106475, 107781, LACM 86301, 111055, USNM 11976, 17333, 18573, 533566, 533568; *Daption capense* AMNH 3126, 8868, 8915, LACM 102367, 102496, 102534, 102571, 102579, 102597; *Diomedea melanophrys* AMNH 3135, 23506, 23564–5, MACN 54409–10; *Eudyptes chrysocome chrysocome* AMNH 5398, 5972, 9173, 26477, LACM 99775; *Eudyptes chrysocome moseleyi* FMNH 291231–3, 312902, 314652, 345115–8; *Eudyptes chrysolophus* AMNH 5964, 26478, FMNH 431779, 339520, LACM 104403, 110995; *Eudyptes pachyrhynchus* AMNH 26509; *Eudyptes robustus* AMNH 27678, *Eudyptes schlegeli* AMNH 5399; *Eudyptes sclateri* BMNH 1952.1.38; *Eudyptula minor* AMNH 5314, 5620, 6957, 11561, FMNH 339521, 106434, 106492, 106505–6, 106997, LACM 90093, 102347–9, 102351, 102353–4, 103167–8, 103938; USNM 560233, 244884; *Gavia stellata* AMNH 4974, 5971, 12905, 24132, LACM 86316, 90036, 99695, 100736, 101089–90, 112288, 112745, 112747–8, 112751; *Macronectes giganteus* AMNH 1634, 5400, LACM 102362–3, 103782, 104882, MACN 1655a, 4474a; *Megadyptes antipodes* AMNH 5613, 5615; *Oceanites oceanicus* AMNH 1357, 16599, LACM 102519, 102553, 102590, 103972, 104105, 104108–9, 104610; *Oceanodroma leucorhoa* AMNH 22019, 22032, LACM 18127, 18129, 20081, 86402, 104314, 104316, 107468, 107969; *Pachyptila desolata* AMNH 3119, 4145, LACM 102501–2, 102510, 102522, 102532, 104299, 106728–9; *Pelecanoides urinatrix* AMNH 16043, FMNH 339530; *Phoebastria palpebrata* LACM 102361; *Procellaria aequinoctialis* AMNH 1638, 8929, LACM 101822, 102261, 102381–2, 103767, 104102, 110997; *Pterodroma incerta*

AMNH 3120, 4693; *Puffinus griseus* AMNH 2902, 23554, LACM 86374, 103648, 103786–7, MACN 68380; *Pygoscelis adeliae* AMNH 26162–3, 26474–6, FMNH 96173, 104041, 339519, 378439, 104213–4, 106733, LACM 101721, 101722, USNM 346811, 490096, 554802, 554822; 554846; *Pygoscelis antarctica* AMNH 26158–9; 26160–1, FMNH 104215–7, 390994; *Pygoscelis papua* AMNH 3191, 4361, 5766, 22679, 26164, FMNH 315111, 330150–4, 339516–8, 344864, 345119; *Spheniscus demersus* AMNH 1310, 1625, 3875, 4069, 10898, 10926, 12782, 22678, FMNH 289829, 291343, 290227, 291234, 375397, 378685, 378754, 104173, 104434, LACM 111061; *Spheniscus humboldti* AMNH 4920, 26165, FMNH 330157, 339522–5, 339527–9, LACM 18473, 18498, 88834; *Spheniscus magellanicus* AMNH 823, 8826, 22677, 26479, 26481, FMNH 379141, LACM 90632, 101723, MACN 54412, 54682–3, 54685; *Spheniscus mendiculus* AMNH 3648, 3772, FMNH 105189, 105390, 105405, 105586, LACM 16055, 18653, 86303–4, 89906.

3. Oological specimens: *Aptenodytes patagonicus* AMNH 5843, 13389–91, 13547–8, 15536; *Daption capense* AMNH 6326, 13444–5; *Eudyptes chrysocome* AMNH 13392, 13412–5; *Eudyptes chrysolophus* AMNH 17297, 17301; *Eudyptes robustus* AMNH 17217; *Eudyptula minor* AMNH 5846; *Gavia stellata* AMNH 39, 42, 44, 46, 6288; *Macronectes giganteus* AMNH 6130, 6136, 13438, 13440, 13555; *Oceanites oceanicus* AMNH 13497 [type]; *Oceanodroma leucorhoa* AMNH 6329, 15537; *Pachyptila desolata* AMNH 13464, 14572–3, 14576; *Pelecanoides urinatrix* AMNH 13513–4; *Phoebastria palpebrata* AMNH 6709–10, 13437; *Procellaria aequinoctialis* AMNH 13456, 13461–2; *Puffinus griseus* AMNH 3034, 5858, 6308, 13489–90; *Pygoscelis antarctica* AMNH 13411; *Pygoscelis adeliae* AMNH 5844, 13410; *Pygoscelis papua* AMNH 13393–6, 13400, 13549–51; *Spheniscus demersus* AMNH 17477; *Spheniscus magellanicus* AMNH 13416–9, 13604; *Spheniscus humboldti* AMNH 13603.

4. Fossil specimens: *Paraptentodytes antarcticus* AMNH 3338, BMNH A591.

## APPENDIX 2

### LIST OF CHARACTERS USED IN THE PRESENT STUDY

List is modified from Bertelli and Giannini (2005). We excluded their character 137, as additional study indicates variation renders the character noninformative. We added one new character (120) from Mayr (2005). Where coding modifications were made, we provide comment in the character description. Full character description, discussion of sources, and illustrations are

given in Bertelli and Giannini (2005). The following characters are considered ordered: 4, 5, 8, 16, 23, 29, 31, 35, 36, 39, 41, 48, 53, 70, 77, 80, 82, 87, 90, 93, 96, 98, 109, 113, 114, 119, 127, 135, 136, 145, 149, and 153.

### INTEGUMENTARY CHARACTERS

#### *Bill (Rostrum)*

0. Tip of maxilla (*rostrum maxillare*): hooked (0); unhooked (1).

1. Tip of mandible (*rostrum mandibulare*): pointed (0); slightly truncated (1); strongly truncated, squared off (2); procellariiform-like (3).
2. Longitudinal grooves on the base of the culmen: absent (0); present (1).
3. Longitudinal grooves on the base of latericorn and ramicorn: absent (0); present (1).
4. Feathering of maxilla (*rostrum maxillare*), extent: totally unfeathered (0); slightly feathered, less than half the length of maxilla (1); feathering that reaches half the length of maxilla (2); feathering surpassing half the length of maxilla (3).
5. Ramicorn, inner groove at tip: absent (0); present and single (1); present and double (2).
6. Orange or pink plate on ramicorn: absent (0); present (1).
7. Plates of rhamphotheca, inflated aspect: absent (0); present (1).
8. Gape (*rima oris*), aspect: not fleshy (0); margin narrowly fleshy (1); margin markedly fleshy (2).
9. Ramicorn color pattern: black (0); reddish (1); pink (2); yellowish (3); orange (4); green (5); blue (6).
10. Latericorn and ramicorn, light distal mark: absent (0); present (1).
11. Latericorn color: black (0); red (1); orange (2); yellow (3); green (4); blue (5).
12. Culminicorn color: black (0); red (1); orange (2).
13. Maxillary and mandibulary *unguis*, color: black (0); red (1); yellow (2); green (3); bluish gray (4).
14. Bill of downy chick, color: dark (0); reddish (1); pale, variably horn to yellowish (2); bluish (3).
15. Bill of immature, color: dark (0); bicolored reddish and black (1); red (2); yellowish (3); grayish (4).
16. Nostril tubes: absent (0); present in chick (1); present in adult (2).
17. External nares: present (0); absent (1).

*Iris (regio orbitalis: oculus [organa sensuum])*

18. Iris color: dark (0); reddish-brown (1); claret red (2); yellowish (3); white (4); silvery gray (5).

*Feathers (Pennae)*

19. Scalelike feathers: absent (0); present (1).
20. Rhachis of contour feathers: cylindrical (0); flat and broad (1).
21. Rectrices: forming a fan functional for steering (0); not (1).
22. Remiges: differentiated from contour feathers and specialized for flight propulsion (0); indistinct from contour feathers (1).

23. Apterina: present (0); absent (1).
24. Molt of contour feathers: gradual (0); simultaneous (1).

*Adult plumage*

25. Yellow pigmentation in crown feathers (*pileum*): absent (0); present (1).
26. Head plumes (*crista pennae*): absent (0); present (1).
27. Head plumes (*crista pennae*), aspect: compact (0); sparse (1).
28. Head plumes (*crista pennae*), aspect: heading upward (0); heading backward, not drooping (1); heading backward, drooping (2).
29. Head plumes (*crista pennae*), position of origin: at base of bill close to gape (0); on the recess between latericorn and culminicorn (1); on forehead (2).
30. Head plumes (*crista pennae*), color: yellowish (0); orange (1).
31. Nape (*occiput*), crest development: absent (0); slightly distinct (1); distinct (2).
32. Periocular area (*regio orbitalis*), color: black (0); white (1); yellow (2); bluish gray (3).
33. Fleshy eyering (*regio orbitalis*): absent (0); present (1).
34. White eyering (*regio orbitalis*): absent (0); present (1).
35. White eyebrow (*regio orbitalis, supercilium*): absent (0); narrow, from postocular area (1); narrow, from preocular area (2); wide, from preocular area (3).
36. Loreal area (*lorum*), aspect: feathered (0); with spot of bare skin in the recess between latericorn and culminicorn (1); with spot of bare skin contacting eye (2); bare skin extending to the base of bill (3).
37. Auricular patch (*regio auricularis*): absent (0); present (1).
38. Throat pattern (*jugulum*): black (0); white (1); yellowish (2); irregularly streaked (3); with chinstrap (4).
39. Collar: absent (0); at most slight notch present (1); present, diffusely demarcated (2); black, strongly demarcated (3).
40. Breast (*pectus*), golden in color: absent (0); present (1).
41. Dorsum color: black (0); dark bluish gray (1); light bluish gray (2).
42. Black marginal edge of dorsum between lateral collar and axillary patch (axilla), contrasting with dorsum: absent (0); present (1).
43. Black dots irregularly distributed over white belly (*venter*): absent (0); present (1).
44. Flanks (*ilia*), dark lateral band reaching the breast (*pectus*): absent (0); present (1).

45. Distinct dark axillary patch of triangular shape (*axila*): absent (0); present (1).
46. Flanks (*ilia*), extent of dorsal dark cover into the leg: incomplete, not reaching tarsus (0); complete, reaching tarsus (1).
47. Rump (*pyga*): indistinct from dorsum (0); distinctly whitish (1).
48. Tail length (*cauda*): short, the quills barely emerge from the rump (0); medium, the quills are distinctly developed but do not surpass the feet extended caudally (1); long, the quills surpass the feet extended caudally (2).
49. Outer rectrices, color: same as inner rectrices (0); lighter than inner rectrices (1).
50. White line connecting leading edge of flipper with white belly (*venter*): absent (0); present (1).
51. Flipper (*ala* [*membrum thoracicum*]), upper-side, light notch at base: absent (0); present (1).
52. Leading edge of flipper (*ala* [*membrum thoracicum*]), pattern of upper-side: black (0); white (1).
53. Leading edge of flipper (*ala* [*membrum thoracicum*]), pattern of underside: white (0); incompletely dark (1); completely dark and wide (2).
54. Flipper (*ala* [*membrum thoracicum*]), underside, dark elbow patch: absent (0); present (1).
55. Flipper (*ala* [*membrum thoracicum*]), underside, tip pattern: immaculate (0); patchy, in variable extent (1); small circular dot present (2).  
*Immature plumage*
56. White eyebrow (*supercilium*): absent (0); present (1).
57. Throat pattern (*jugulum*): black (0); mottled (1); white (2); brown (3).
58. Flanks (*ilia*), dark lateral band: absent (0); present (1).

#### *Natal plumage (neossoptilus)*

59. Chicks hatch almost naked: no (0); yes (1).
60. Dominant color pattern of first down: pale gray (0); distinctly brown (1); bicolored, dark above and whitish below (2); uniformly blackish gray (3).
61. Dominant color pattern of second down: pale gray (0); distinctly brown (1); bicolored, dark above and whitish below (2); uniformly blackish gray (3).
62. Chick, second down, collar: absent (0); present (1).

#### *Feet (podoteca)*

63. Feet (*pedes*), dorsal color: dark (0); pinkish (1); orange (2); white-flesh (3); blue (4).

64. Feet (*pedes*), dark soles: absent (0); present (1).
65. Feet (*pedes*), *unguis digiti*: flat (0); compressed (1).

#### BREEDING CHARACTERS

66. Clutch size: two eggs (0); one egg (1).
67. Incubatory sac: absent (0); present (1).
68. Nest: no nest, incubation over the feet (0); nest placed underground, either burrowed on sand or inside natural hollow or crack (1); open nest, a shallow depression on bare ground or in midst of vegetation (2).
69. Size of first egg relative to the second egg: similar (0); dissimilar, first smaller (1); dissimilar, second smaller (2).
70. Crèche: absent (0); small, 3–6 birds (1); typical, conformed by dozens to hundreds of immatures (2).
71. Eggs, shape: oval (0); conical (1); spherical (2).
72. Ecstatic display: absence (0); presence (1).

#### OSTEOLOGICAL CHARACTERS

##### *Cranium*

73. Basioccipital, subcondylar fossa (*os basioccipitale, fossa subcondylaris*): absent to shallow (0); deep (1).
74. Supraoccipital, paired grooves for the exit of the *v. occipitalis externa* (*os supraoccipitale, sulci venae occipitalis externae*): poorly developed (0); deeply excavated (1). In some individuals of *Pygoscelis papua* we found variation in the development of the grooves, and so changed the coding for this taxon to polymorphic.
75. Frontal, salt-gland fossa (*os frontale, fossa glandulae nasalis*), lateral supraorbital shelf of bone: absent (0); present (1).
76. Squamosal, temporal fossa (*os squamosum, fossa temporalis*), size: less extensive, both fossae separated by considerable cranial surface (at least the width of the cerebellar prominence) (0); more extensive, fossae meeting or nearly meeting at midline of the skull (1).
77. Squamosal, temporal fossa (*os squamosum, fossa temporalis*), depth of posterior region: flat (0); shallow (1); greatly deepened (2).
78. Squamosal (*os squamosum*), development of the lateral foramen *rami occipitalis arteriae ophthalmicae externae* in the caudoventral area of the *fossa temporalis* (near the *crista nuchalis*): small or vestigial (0); well developed (1).
79. Orbit (*orbita*), *fonticuli orbitocraniales*: small or vestigial (0); broad and conspicuous openings (1).

80. Ectethmoid (*os ectethmoidale*): absent (0); weakly developed, widely separated from the lacrimal (1); well developed, contacting or fused to the lacrimal (2).
81. Lacrimal (*os lacrimale*): unperforated (0); perforated (1).
82. Lacrimal (*os lacrimale*): reduced, concealed in dorsal view (0); exposed in dorsal view, without a prominent orbital process (*proc. orbitalis*) (1); highly exposed dorsally, with a prominent orbital process (2).
83. Lacrimal, dorsal border: closely applied to the frontal (0); separated by a wide split from the frontal (1).
84. Nasal cavity, external naris (*cavum nasi, apertura nasi ossea*), caudal margin: extended caudal to the rostral margin of the *fenestra antorbitalis* (0); not extended caudal to the rostral margin of the *fenestra antorbitalis* (1).
85. Nasal cavity (*cavum nasi, pila supranasalis*): slender, slightly constricted laterally (0); wide throughout its length (1).
86. "Basitemporal plate" (*lamina parasphenoidalis*), dorsoventral position with respect to the occipital condyle: ventral to the level of the condyle (0); at the level of the condyle (1); dorsal to the level of the condyle, surface depressed (2).
87. Basipterygoid process: absent (0); vestigial or poorly developed (1); well developed (2).
88. Eustachian tubes (*tuba auditiva*): open or very little bony covering near the posterior end of the tube (0); mostly enclosed by bone (1). We found the eustachian tube to be open in some individuals of *Pygoscelis papua* and *Pygoscelis antarctica*, so changed the codings for these species to polymorphic.
89. Pterygoid (*os pterygoideum*), shape: elongated (0); broad, triangular-shaped (1).
90. Palatine (*os palatinum*), *lamella choanalis*: curved and smooth plate, slightly differentiated from main palatine blade (0); ridged, distinct from main blade by a low keel (1); extended ventrally, forming the *crista ventralis* (2).
91. Vomer (*vomer*): laterally compressed vertical laminae, free from palatines (0); ankylosed with palatines (1).
92. Facial foramen (*ossa otica, fossa acustica interna, foramen n. facialis*): absent (0); present (1).
93. Jugal arch (*arcus jugalis*), bar shape in lateral view: straight (0); slightly curved (1); ventrally bowed (2); strongly curved, sigmoid shape (3).
94. Jugal arch (*arcus jugalis*), dorsal process: absent (0); present (1).
95. Premaxilla (*os premaxillare*), naso-premaxillary suture: visible (0); obliterated (1).
96. Quadrate, otic process (*os quadratum, proc. oticus*), ventral border, process for attachment of the *M. adductor mandibulae externus, pars profunda* (Hofer, 1950): absent (0); present as a ridge (1); present as a tubercle (2).
97. Tomial edge (*crista tomialis*): plane of tomial edge approximately at the level of the "basitemporal plate" (*lamina parasphenoidalis*) (0); dorsal to the level of the basitemporal plate (1).
98. Mandible, coronoid process (*mandibula, processus coronoides*), position on the dorsal margin of the mandible with respect to the caudal fenestra (*fenestra mandibulae caudalis*): markedly anterior (0); on the anterior end of the fenestra (1); posterior (2).
99. Mandible, rostral fenestra (*mandibula, fenestra mandibulae rostralis*): imperforated or small opening (0); well developed (1).
100. Mandible, caudal fenestra (*mandibula, fenestra mandibulae caudalis*): open, can be seen through from the medial or lateral aspects (0); nearly or completely concealed by the *os spleniale* medially, that is, fenestra not visible in the medial aspect (1).
101. Mandible, mandibular ramus (*mandibula, ramus mandibulae*): depth subequal over entire ramus (0); noticeably deepening at midpoint (1).
102. Mandible, dentary (*mandibula, os dentale*), posterior border divided into: one limb (0); two limbs (1).
103. Mandible, dentary, length of dorsal edge (*ossa mandibulae, os dentale, margo dorsalis*) relative to mandibular ramus length in lateral view: markedly more than half the length of ramus (0); approximately half the length of ramus (1).
104. Mandible, articular, medial process (*os articulare, proc. medialis mandibulae*): not hooked (0); hooked (1).
105. Mandible, angular, retroarticular process (*mandibula, os angulare, proc. retroarticularis*), aspect in dorsal view in relation to the articular area with the quadrate (area between the lateral condyle [*condylus lateralis*] and medial condyle [*condylus medialis*]): broad, approximately equal to the articular area (0); moderately long, narrower than the articular area (1); very long, longer and narrower than the articular area (2).
106. Mandible, angular (*mandibula, os angulare*), aspect in dorsal view: sharply truncated caudally (0); caudally projected, forming the retroarticular process (*proc. retroarticularis*) (1).
107. Mandible, caudal fossa (*mandibula, fossa caudalis*): shallow (0); deep (1).



108. Atlas (*atlas*), *proc. ventralis corporis*: absent or slightly developed (0); well developed, high and prominent ridge on the dorsal surface of the *corpus atlantis* (1).
109. Transition to free cervicothoracic ribs (*costae incompletae*) arrives at: 13th cervical vertebrae (0); 14th cervical vertebrae (1); 15th cervical vertebrae (2).
110. Cervical vertebrae (*vertebrae cervicales*), elongated dorsal process (*processus spinosus*) on the sixth cervical vertebra: absent (0); present (1).
111. Cervical vertebrae (*vertebrae cervicales*), transverse processes (*processus transversus vertebrae*) in last five cervical vertebrae: not elongated laterally (0); greatly elongated laterally (1).
112. Cervical vertebrae (*vertebrae cervicales*), transverse processes (*processus transversus vertebrae*) of vertebrae 12–13: laterally oriented (0); deflected dorsally (1).
113. Caudal vertebrae (*vertebrae caudales*): seven (0), eight (1), nine (2).
114. Ribs, uncinat processes (*costae, proc. uncinatus*): elongate, narrow (0), wide, spatulate (1), wide, bifurcated (2).
115. Sternum, external spine (*sternum, spina externa rostri*): present (0); absent (1).
116. Sternum, furcular facet (*sternum, facies articularis furculae*) projects as a distinctive process: absent (0); present (1).
117. Clavicle, furcular process (*clavicula, apophysis furculae*): absent, or short bladlike projection (0); knoblike process (1); long process (2). The original formulation of this character included four states. After observing additional specimens, we note that the presence or absence of a low, bladlike furcular process is variable in the majority of extant species, and have so combined two character states from the previous matrix into a single state.
118. Scapula, blade, caudal half (*scapula, corpus scapulae, extremitas caudalis*): flattened and usually bladlike (0); paddle-shaped (1).
119. Coracoid, medial margin (*coracoideum, margo medialis*) fenestrate lamella: complete (0); incomplete (1); absent (2).
120. Coracoid, *foramen nervi supracoracoidei*: present (0), absent (1). This character is modified from Mayr (2004, character 29).
121. Coracoid, sternal end (*coracoideum, extremitas sternalis coracoidei*): wide (0); narrow (1).
122. Forelimbs (*ossa alae*), strongly flattened: absent (0); present (1).
123. Humerus, pneumatic fossa (*humerus, fossa pneumotricipitalis*), aspect: small with pneumatic foramina (0); without pneumatic opening, moderate size (1); without pneumatic opening, of great size and deep (2).
124. Humerus, head (*humerus, caput humeri*): very developed and reniform, ventrally directed: absent (0); present (1).
125. Humerus, pneumatic fossa (*humerus, fossa pneumotricipitalis*), subdivision into cavities: single (0); bipartite (1).
126. Humerus, development of dorsal supracondylar process (*humerus, proc. supracondylaris dorsalis*): absent (0); compact tubercle (1); very long process (2).
127. Humerus, deltoid crest, impression for attachment of pectoral muscle (*humerus, crista deltopectoralis, impressio m. pectoralis*): superficial or shallow groove (0); deep oblong fossa (1).
128. Humerus (*humerus*), distal end, ventral border with “trochlear process” (caudal-most process-like crest at the epicondylus ventralis caudally bordering the *sulcus humerotricipitalis*): present (0); absent (1).
129. Humerus (*humerus*), proximal-most “trochlear process”: extends beyond the humeral shaft (0); does not extend beyond the humeral shaft (1). After examining additional specimens, we note variation in the extension of the proximal-most “trochlear process” in *Spheniscus demersus* and have changed the coding for this taxon to polymorphic.
130. Phalanges of manus, free pollex (*ossa digitorum manus, phalanx digiti alulae*): absence (0); presence (1).
131. Phalanges of manus, phalanx digit III (*ossa digitorum manus, phalanx digiti minoris*), proximal process: absent (0); present (1).
132. Phalanges of manus (*ossa digitorum manus, phalanx*): short (0); long (1).
133. Pelvis (*pelvis et os coxae*), size of ilio-ischiatic fenestra (*foramen ilioischadicum*) in relation to acetabulum (*foramen acetabuli*): smaller (0); similar in size or larger (1).
134. Pelvis, ischio-pubic fenestra (*pelvis et os coxae, fenestra isquiopubica*): very wide and closed at its caudal end (0); slitlike and open at its caudal end (1).
135. Ischium (*ischium*), most caudal extent in relation to postacetabular ilium (*ala postacetabularis ilii*): ischium shorter than postilium (0); ischium projects slightly beyond the postilium (1); ischium produced far backward postilium (2).
136. Femur, patella (*femur, patella*), *sulcus m. ambiens*: shallow groove (0); deep groove (1); perforated (2).
137. Tibiotarsus, patellar crest (*tibiotarsus, cristae patellaris*): greatly enlarged (0); slightly developed (1).

138. Tarsometatarsus (*tarsometatarsus*): slender, proximodistal length much greater than mediolateral width (0); very stout, mediolateral width nearly equal to proximodistal length.
139. Tarsometatarsus (*tarsometatarsus*), blood vessel foramen located on *fossa para hypotarsalis medialis*: absent (0); present (1).
140. Tarsometatarsus, medial proximal foramen (*tarsometatarsus, foramina vascularia proximalia*) opens lateral to medial crest (*crista medialis hypotarsi*): absent (0); present (1).
141. Tarsometatarsus, hypotarsus, tendinal canals (*tarsometatarsus, hypotarsus, canales hypotarsi*): present (0); absent (1).
142. Tarsometatarsus (*tarsometatarsus*), *tuberositas m. tibialis cranialis*: flat (0); raised (1).

#### MYOLOGICAL CHARACTERS

143. *M. latissimus dorsi, pars cranialis*, accessory slip: absent (0); present (1).
144. *M. latissimus dorsi, pars cranialis* and *pars caudalis*: separated (0); fused (1).
145. *M. latissimus dorsi, pars metapagialis*, development: wide (0); intermediate (1); narrow (2).
146. *M. serratus profundus*, cranial fascicle: absent (0); present (1);
147. *M. deltoideus, pars propatagialis*, subdivision in superficial and deep layers: undivided (0); divided (1).
148. *M. deltoideus, pars major*: triangular or fan-shaped (0); strap-shaped (1).
149. *M. deltoideus, pars major, caput caudale*: short (0); intermediate (1); long (2).
150. *M. deltoideus, pars minor*, origin on the clavicular articulation of the coracoid: absent (0); present (1).
151. *M. ulnometacarpalis ventralis*: absent (0); present (1).
152. *M. iliiochantericus caudalis*: narrow (0); wide (1).
153. *M. iliofemoralis*, origin: tendinous (0); mostly tendinous (1); mostly fleshy (2); totally fleshy (3).
154. *M. flexor perforatus digitis IV, rami II–III*: free (0); fused (1).
155. *M. flexor perforatus digitis IV, rami I–IV*: free (0); fused (1).
156. *M. flexor perforatus digitis IV*, insertion of middle *rami*: on phalanx 3 (0); on phalanx 4 (1).
157. *M. latissimus dorsi, pars caudalis*, additional origin from dorsal process of vertebrae (spinous process of Schreiweis, 1982): absent (0); present (1).

#### DIGESTIVE TRACT

158. Mouth, oral mucosa (*bucca, tunica mucosa oris*), buccal papillae group (sensu Watson, 1879) on the medial surface of the lower jaw (*ramus mandibularis*) at the level of the rictus: small number of rudimentary papillae with no clear arrangement (0); two clear rows of short conical papillae (1); large, elongated papillae with no clear arrangement (2). In a previous analysis (Bertelli and Giannini, 2005) we considered only the presence or absence of the buccal papillae. We have here expanded this character to reflect variation within Sphenisciformes.



